On the Efficiency, Exergy Costs and CO_2 Emission Cost Allocation for an Integrated Syngas and Ammonia Production Plant

Daniel Flórez-Orrego[a], Silvio de Oliveira Junior [b]

Department of Mechanical Engineering, Polytechnic School, University of Sao Paulo, Sao Paulo, 05508-900, Brazil. [a]daflorezo@usp.br CA, [b]soj@usp.br

Abstract:

This paper presents an exergy and environmental assessment of a 1000 metric t/day ammonia production plant based on the steam methane reforming (SMR) process, including the syngas production, purification (CO_2 capture) and compression units, as well as the ammonia synthesis and purge gas treatment. An integrated heat recovery system produces power and steam at three pressure levels, besides exporting hot water, CO_2 and fuel gas, with no additional heat or power consumption being required. Two configurations for ammonia refrigeration process (-20ºC) are compared in terms of power consumption. Exergy cost data for upstream processing stages of natural gas is used to calculate the extended exergy cost of the products of the plant, namely ammonia, CO_2 and fuel gas. Moreover, an appropriated methodology is employed to properly allocate the renewable and non-renewable exergy costs, as well as the CO_2 emissions of the reforming, shift and furnace stack among the products of the plant. By considering that the cost reduction of the combustion gases is a linear function of the exergy flow rate reduction in each component of the heat recovery system, an improved allocation of the CO_2 emission cost along the convection train is performed. A breakdown of the total exergy destruction rate of the plant (136.5MW) shows that about 59% corresponds to the reforming process followed far behind by the ammonia synthesis and condensation (18.3%) and the gas purification units (13.2%). The overall exergy efficiency of the ammonia plant is calculated as 66.36%, which is enhanced by recovering the hydrogen-rich and fuel gases in the purge gas treatment process. The total and non-renewable exergy costs and CO2 emission cost of the ammonia produced are calculated as 1.7950 kJ/kJ and 0.0881 kg_{CO2}/MJ, respectively. In addition, a rational exergy cost of 1.6370 kJ/kJ and CO_2 emission cost of 0.0821 kg_{CO2}/MJ are allocated to the CO_2 gas, which can be supplied as feedstock to an associated chemical plant (urea, methanol, polymers, etc.).

Keywords:

Ammonia Production; Renewability; Exergy Cost; CO2 Emissions; Exergy Efficiency

1. Introduction

Some fundamental mineral nutrients limiting the vegetal growing, e.g. carbon and oxygen, can be easily obtained by the plants through the soil and the surrounding air. Others, like nitrogen, must be first fixed into plant-accessible forms, e.g. synthetic nitrogen fertilizers (SNF)[1] [1], which currently are thought to be responsible for at least 50% of crops yield [2]. In fact, alongside the population growth, the world nitrogen fertilizers demand (as N) is expected to increase more than 5.8 million of metric tons between 2014 and 2018 [3], with the largest annual growth rate in the Americas expected in Latin America (3.27%), especially in Brazil [4]. However, regardless of the large production volumes, the national fertilizer industry has not enough capacity for supplying the total demand and, thus, more than 60% of the national SNF consumption must be imported [5]. The fact that the growth in demand for fertilizers has surpassed Brazilian production capacity makes the country vulnerable to variations in prices in the international markets, natural gas prices, shipping costs and logistical problems at Brazilian ports [6]. Technological and economic lags are partly, but not exclusively, due to existent plants still based on low efficiency technologies. Aiming to reduce

[1]The products classified in the category of SNF include ammonia, urea, ammonium nitrate and some others straight (calcium nitrate, ammonium sulfate, etc.) and complex (ammonium phosphates, nitro-phosphates, etc.) fertilizers.

foreign dependence to only 13% in 2020 [7], further investments in the construction of new plants or revamping old ones are envisaged [5, 7-9]. Besides, considering that steam methane reforming (SMR) is the most cost-efficient technology for ammonia synthesis due to the relative gas availability, higher H_2/CO ratios and lower energy use [10]; recent natural gas discoveries in the Pre-salt region may also help to stabilize SNF production, to decrease the external dependence and the internal price fluctuation. Yet, the technological and logistical adaptations to extract that natural gas are still expensive [11]. Aside from those economic aspects, the environmental performance of chemical processes also became a growing awareness in industry in the last decades and SNF plants have continuously deserved more legal surveillance [12]. However, in spite of the existing regulatory policies, unclearly defined limits render the impact quantification difficult and in some cases the mitigation unprofitable (e.g. in post-combustion CCS for flue stacks) [8]. For instance, if ammonia is used for urea manufacture, then a fraction of the process by-products such as CO_2 gas from desorber vent are no more emitted to the atmosphere, but recovered and recycled as feedstock, whereas liquid process condensates are typically purified and recycled, decreasing both the energy consumption and wastes, which should be accounted for in the whole environmental analysis.

Over the last few years, SNF technology has undergone radical developments in terms of both design and equipment. The efforts have mainly focused on reducing power and feedstock consumption [13], improving the heat recovery network [14-20], minimizing stack losses, cutting energy consumption for CO_2 removal [21-23] and designing better and more active catalysts (Ru-based) [13, 24-27]. Exergy and environmental analyses on SMR process, ammonium nitrate and nitric acid plants have also been performed [28-31]. More recent studies carried out the thermo-environomic analysis of ammonia production [32]. Notwithstanding the level of energy integration and recent developments in modern ammonia plants, the specific exergy consumption has not been reduced radically so far. In fact, it is noteworthy that the minimum theoretical exergy consumption in ammonia plants is still much lower (18-21GJ/t_{NH3}) [33] than the best figures reported in the literature (28-31 GJ/t_{NH3}), which vary widely with local conditions and project-specific requirements [13, 31]. Thus, according to The European Roadmap of Process Intensification (PI - PETCHEM), the potential benefits in the ammonia production sector are significant: 5% higher overall energy efficiency for the short/midterm (10-20 years) and 20% higher (30-40 years) for the long term [34]. Clearly, better developments will be subjected to economic aspects, but increasing the efficiency of domestic production's share could be the first step towards the reduction of the large non-renewable exergy consumption and environmental impact that SNF industry is responsible for. Accordingly, in this work, exergy is used to analyze an integrated syngas and ammonia production plant in order to quantify the exergy efficiency and destruction in each unit. Even though energy-based Life Cycle Analyses has been previously reported for the Brazilian SNF scenario [35], neither unit exergy costs nor specific CO_2 emission cost allocation have been performed. Thus, by using an appropriated methodology, the renewable and non-renewable unit exergy costs and the CO_2 emissions, arisen from the combustion furnace, as well as from the reforming and shift reactions in the SMR facilities, are allocated among all the products of the plant. Also, due to the interplay among the various processing units with the heat recovery network and the utilities plants, major attention is given to the exergy cost and CO_2 emission cost allocation in the convection train of the reformer.

2. Methodology

In this work, the exergy method is used for defining indicators to assess the performance of the processes present in an integrated syngas and ammonia production plant. In the following sections, the main definitions, as well as the exergy cost allocation methodology and the efficiency calculation criteria are presented.

2.1. Exergy Calculation

In the last decades, several tools based on the First and Second Laws of Thermodynamics have been developed for defining indicators to assess the performance of chemical and industrial processes. The combination of these two laws led to the concept of *exergy*. Exergy is defined as the maximum available work that can be obtained from a thermodynamic system through its interaction with the environment by means of reversible processes until the equilibrium state (mechanical, thermal and chemical) with the environment components is attained [36]. In this work, the reference ambient parameters (pressure, temperature and composition) considered for calculating exergy correspond to those reported by [36]. Total exergy accounts for potential (P), kinetic (K), thermo-mechanical or physical (PH) and chemical (CH) exergy components, each one calculated by using Eqs. (1-4), respectively:

$$B^K = 1/2\, m\upsilon^2 \tag{1}$$

$$B^P = mgz \tag{2}$$

$$B^{PH} = \int mc_p dT + \int \left[V - T\left(\frac{\partial V}{\partial T}\right)_P \right] dP - T_O \left[\int mc_p \frac{dT}{T} - \int \frac{V}{T} dP \right] \tag{3}$$

$$B^{CH} = N_{mix} \bar{b}^{CH} = N_{mix} \left[\sum_i y_i\, b_i^{CH} + R_u T_O \sum_i y_i\, \ln \gamma_i\, y_i \right] \tag{4}$$

The terms y_i and γ_i in Eq. (4) are the mole fraction and the activity coefficient of component *i* in the mixture, respectively, and b_i^{CH} is the standard chemical exergy of component i. Equation (4) is especially useful when calculating the chemical exergy of gaseous fuels whose chemical composition can be readily determined and thermochemical data for the components are thoroughly reported. However, solid and liquid industrial fuels and other substances are often solutions of numerous chemical compounds of, usually, unknown nature. Therefore, by assuming that the ratio of chemical exergy to the lower heating value ($\varphi = b^{CH}/LHV$) is the same for pure chemical substances having the same ratios of chemicals constituents (H/C, O/C, N/C), Szargut and Styrylska derived correlations expressing the dependence of φ on those atomic ratios [36].

Since the integrated syngas and ammonia production plants are complex multi-component/multi-phase systems, Aspen HYSYS® simulation software is used to determine the thermodynamic and transport properties of each flow by using Peng-Robinson and Soave-Redlich-Kwong equations of state, as well as proprietary Acid Gas® fluid package. Additionally, as the previous tool only provides the result of mass, energy and entropy balances, thus molar physical and chemical exergies of each stream must be calculated by programming *scripts* as *user defined functions* in Aspen Hysys® environment [37].

2.2. Exergy Cost Balances

As long as exergy stands for the useful energy required for an economic activity to be accomplished, it is reasonable to evaluate the cost of the energy on the basis of its exergy content [38]. Besides, as exergy can be considered as measure of the departure of the environmental conditions, it also serves as an indicator of environmental impact, taking into account both the efficiency of supply chain (from primary exergy inputs) and the efficiency of the production processes (e.g. syngas and ammonia plants) [39]. In this way, exergoeconomy can be used to rationally distribute the exergy costs and CO_2 emission cost among the products and by-products (hot water, CO_2 gas, fuel gas, etc.) of a single ammonia plant. Based on the thermoeconomy theories [40-46], the authors [47-51] have shown that exergoeconomy provides an opportunity to quantify the renewable and non-renewable, specific exergy consumption; to properly allocate the associated CO_2 emissions among the streams of a given production route; as well as to determine the overall exergy conversion efficiency of the production processes. According to [49-51], the non-renewable unit exergy cost (c_{NR}) [kJ/kJ] is defined as the rate of non-renewable exergy necessary to produce one unit of exergy rate/flow rate of a substance, fuel, electricity, work or heat flow, whereas the Total Unit Exergy Cost (c_T) includes the Renewable (c_R) and Non-Renewable Unit

Exergy Costs. Analogously, the CO_2 emission cost (c_{CO2}) [$kmol_{CO2}/kJ$] is defined as the rate of CO_2 emitted to obtain one unit of exergy rate/flow rate. By considering the control volume embodying each unit operation (Fig. 1), exergoeconomy balances of total and non-renewable exergy costs can be written as in Eqs. (1-2):

$$\sum_j c_{T,P}^j B_{T,P}^j = \sum_i c_{T,F}^i B_{T,F}^i \tag{1}$$

$$\sum_j c_{NR,P}^j B_{NR,P}^j = \sum_i c_{NR,F}^i B_{NR,F}^i \tag{2}$$

where B stands for the exergy rate/flow rate of the exergy flow consumptions (or fuels, F) and products (P) of the respective control volume. Analogously, the CO_2 emission cost balances can be written as in Eq. (3), where the direct CO_2 emissions, either produced by burning the fuel consumptions i or arisen from the chemical reactions of the supplied fuels (e.g., steam reforming, shift, etc.), are accounted for in the $M_{CO_2,F}^i$ and $M_{CO_2,Rxn}$ terms [$kmol_{CO2}/s$], respectively:

$$\sum_j c_{CO_2,P}^j B_{T,P}^j = \sum_i \left(c_{CO_2,F}^i B_{T,F}^i + M_{CO_2,F}^i \right) + M_{CO_2,Rxn} \tag{3}$$

Differently from the unit exergy cost of an external input entering the control volume, which is considered as the unity (or known from previous analysis), in the case of CO_2 emission cost, initial input values are considered equal to zero (or known).

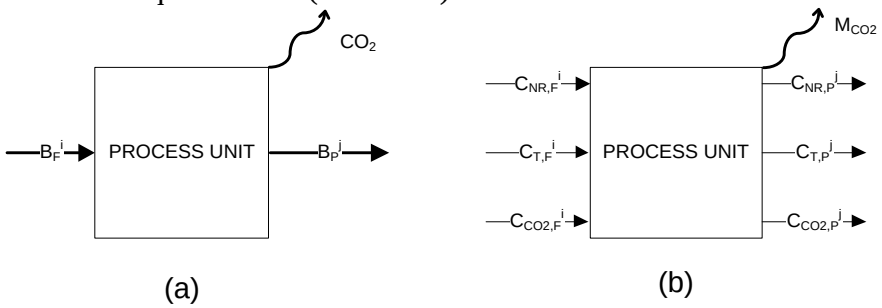

Fig. 1. (a) Exergy flows: fuel inputs (F), product outputs (P); (b) Exergy and CO_2 emission costs.

According to Fig. 2, the integrated syngas and ammonia production plant can be divided into four units, e.g. syngas production (reforming/shift), gas purification (CO_2 removal/methanation), ammonia synthesis (synthesis reaction, refrigeration/condensation, purge gas recovery), and utilities plant (steam and power production, cooling utilities and hot water). These elements are strongly interrelated to each other's operation conditions, affecting simultaneously different sections of the plant concept.

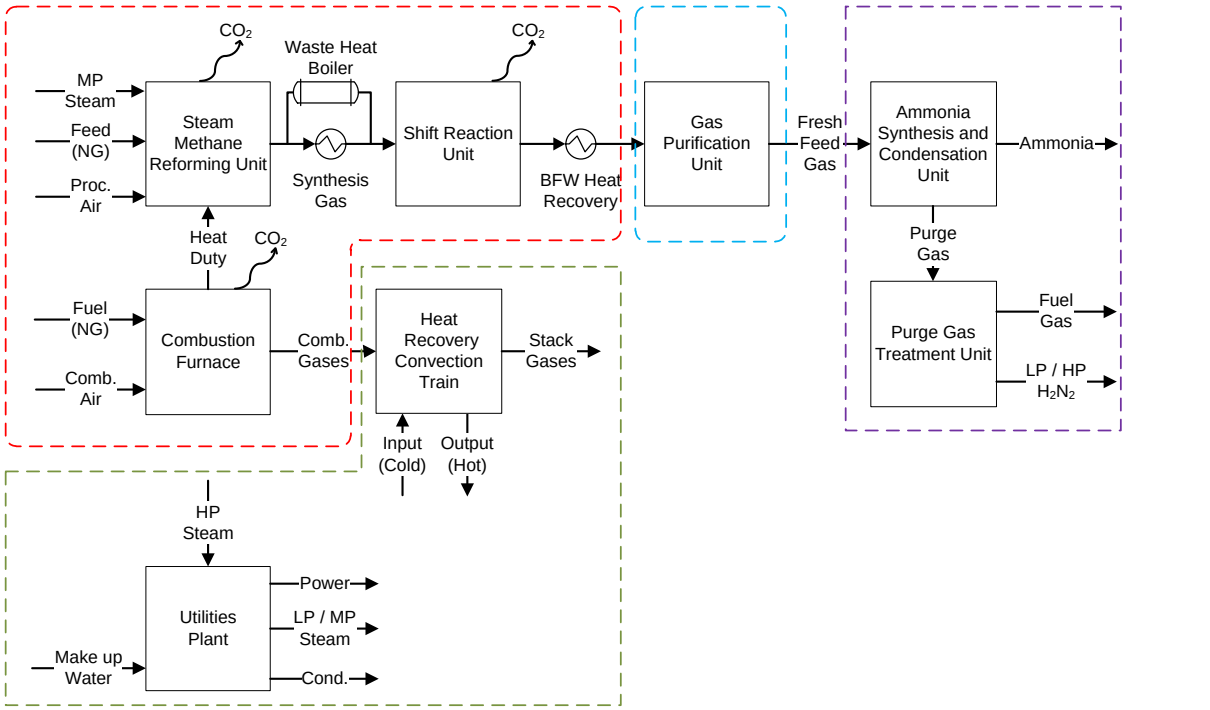

Fig. 2. Simplified layout of the integrated syngas and ammonia production plant.

Due to the large amount of interconnecting flows, an explicit depiction of the integration between streams and exergy flows of each unit would be cumbersome, but it may be still easy matching them by using their names and corresponding numbers through the more detailed layouts of the ammonia plant units, shown in Figures A.1, A.3, 6 and 8. In the following sections, the suitable auxiliary equations for the allocation of the exergy and CO_2 emission costs are developed, particularly among the HRCT and dissipative devices products. These equations are used along with Eqs. (1-3) to calculate the costs related to the useful products.

2.3. Auxiliary equations for unit exergy cost allocation

In the SMR process, natural gas is consumed as fuel in combustion furnace and feedstock in reforming furnace. The purpose of the combustion furnace is to increase the physical exergy of the streams at the expense of their chemical exergy [44]. After the major part of the physical exergy of the combustion gases is delivered to the reforming furnace to address the SMR reaction, the gases continue through the convection train modules (HRCT) where the heat recovery process is performed (Fig. 3). Since the flue stack gases released to the environment are no longer neither thermodynamically nor economically useful, the unit exergy cost and CO_2 emissions cost attributed to them must be zero [41]. On the other hand, according to extraction criterion, if the whole or a part of the exergy input of a given HRCT module is equal to the exergy decrease of the gases that goes through its control volume, then the unit exergy costs of such gases is constant along it ($c^0 = ... = c^k = ... = c^n = \dot{C}^n / B^n$). However, by directly applying this criterion some exergy costs would remain unallocated, which results in a unit exergy cost of the cold rejected gases greater than unity, and thus producing an artificially lower cost for the products of the HRCT [52]. Furthermore, if extraction criterion is still applied but now a zero-value cost is assigned to only the exhaust stream of the HRCT ($\dot{C}^n = 0$), all the costs would be discharged on the product of the last component of the HRCT (hot combustion air), penalizing the hot flue gas production in a non-uniform basis [53, 54]. To overcome this problem, some authors [55] proposed a monetary analysis [$/kJ] in which the unit exergy cost of the hot combustion gases is allocated along the components of a HRSG, linearly proportional to their exergy decrease and by imposing the condition that flue gases exiting the stack of HRSG have zero cost. However, differently from monetary approaches in which unit exergy cost lower than unity has physical meaning, exergy costs lower than unity do not

represent meaningful stream conditions, since the exergy required to produce the stream cannot be lower than the exergy embodied in the stream itself. Aiming to deal with these shortcomings, an abatement fictitious unit can be used to calculate the cost of the "exergy loss" when releasing the flue stack gases to the atmosphere, according to the exergoeconomy balance given in Eq. (4):

$$\dot{C}_{Loss} + \dot{\not{C}}^{0}_{Dead} = c^{n} \cdot B^{n} + \dot{C}_{abat} \tag{4}$$

where the outlet cost flows of such a fictitious unit consist of the cost of flue stack gases at absolute dead state $\dot{C}_{Dead}$ (thus, zero cost) and the cost of exergy loss, $\dot{C}_{Loss}$.

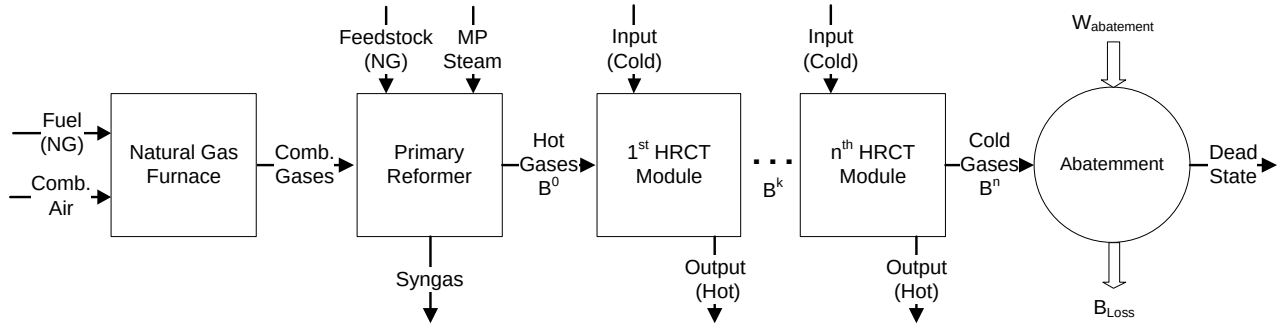

Fig. 3. Representation of the HRCT for unit exergy cost allocation.

The term $\dot{C}_{abat}$ considers the cost of the additional work used in the abatement of the releasing conditions of the cold gases, as in post-combustion carbon capture and storage (PCCS) units. Finally, in other to apportion the total cost of the exergy loss among the product of the *k-th* HRCT component ($\dot{C}^{k}_{Loss}$), a weighting criterion, based on the exergy decrease of the flue stack gases along each component, is adopted:

$$\dot{C}^{k}_{Loss} = \frac{B^{k-1} - B^{k}}{B^{Comb.Gases} - B^{n}} \dot{C}_{Loss} \tag{5}$$

In this way, neither the last HRCT component is overcharged with the total cost of the exergy loss, nor are exergy costs left unallocated to the final products of the HRCT. Even though the chemical exergy fraction of the exergy loss may not be readily available to produce useful work due to current technological restrictions, its contribution is also included for the sake of completeness.

2.4. Auxiliary equations for CO_2 emission cost allocation

Both natural gas burning and SMR process lead to a massive production of direct CO_2 emissions, whose costs must be rationally distributed among the products of the HRCT and the reforming unit. The shift reaction process also produces a large amount of CO_2 emissions, but its allocation is more straightforward than in the two former cases. None of the remaining units of the integrated syngas and ammonia production plant has associated direct CO_2 emissions. Although various approaches have been proposed to deal with carbon taxes on the combined heat and power production (CHP) systems [56-58], they yield different results and, thus far, are not universally accepted or sometimes are inconsistent with thermoeconomy theories. A particular case is the allocation of zero CO_2 emission cost to 'zero' carbon fuels (i.e. from biomass) which clearly ignores the contribution of the fossil inputs at the upstream stages of their supply chain [49, 50]. Another drawback of the proposed methods is that they ignore the quality of energy and focus only on the quantities involved, which might underestimate the share of the emissions allocated to the electrical product. For instance, by considering average efficiencies of both electricity generation (25-50%) and steam production in fired boilers (50-90%), some studies [58] have assumed that the amount of fuel required to generate each unit of electricity is as much as twice the required to generate each unit of heat. Consequently, the carbon intensity of electricity is fixed at twice that of steam, which clearly misleads purchasers of steam, electricity or even of CO_2 to wrongly believe they are buying lower/higher carbon supplies. Other methods, even though showing sound reasoning, seem overly complex in notation, avoiding potential policy makers aware of their benefits. On the other hand,

some works have focused on the decomposition of the CO_2 emissions among the various units of the plant, instead of performing the cost allocation on its streams [59]. Accordingly, in this work, a proposed procedure used for the allocation of CO_2 emission costs, successfully applied to biomass and fossil fuels production [47, 48, 50], highly integrated electricity mixes [49] and comparative assessments of vehicle fuels end-use [60], is adopted. Figure 4 shows the interrelation among the combustion furnace, the primary reformer and the convection train.

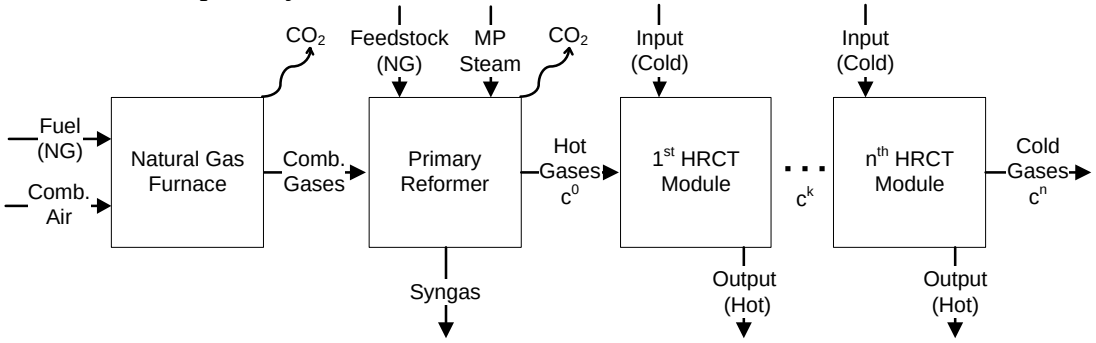

Fig. 4. Heat recovery convection train (HRCT) representation for CO_2 emission cost allocation.

Since the CO_2 emission cost is given in a molar basis ($kmol_{CO2}/kJ$), there is no restriction regarding the minimum positive value that it can assume and, thus, a procedure analogous to that suggested by [55] is performed. Starting from the CO_2 emission costs data [50] of both natural gas (fuel) and preheated combustion air, the CO_2 emission cost of the gases leaving the combustion furnace ('Comb. Gases' in Fig. 4) can be calculated by using Eq.(3). Next, this value along with Eq.(6) is used to calculate the CO_2 emission cost of the hot gas leaving the primary reformer (c^0). In Eq. (6), *k* stands for the "following" flue gas stream (after the *k*-th HRCT module) and *k-1* stands for the "preceding" one ($k = 1-6$). This procedure is iteratively done until the flue gas output of the last component of the HRCT is reached (c^n). The second term of the right-hand side in Eq.(6) imposes the restriction that the CO_2 emission cost of the cold gases exiting the stack of the HRCT is null. Thus, the set of equations given by Eq.(3) together with the auxiliary allocation Eq.(6) allows calculating the CO_2 emission costs of the products of the HRCT.

$$c_{CO_2}^{k} = \left(1 - \frac{B^{k-1} - B^{k}}{B^{Comb.Gas} - B^{n}}\right) c_{CO_2}^{k-1} + \left(\frac{B^{n-1} - B^{n}}{B^{Comb.Gas} - B^{n}} - 1\right) c_{CO_2}^{n-1} \tag{6}$$

Obviously, from the point of view of renewability, it is not practical to reverse the chemical reaction into fuel production to abate the CO_2 emissions. Rather, the CO_2 embodied in the rejected gases can be taken down to a minimal pollution potential in the environment, whilst consuming additional exergy (carbon capture, compression, reinjection, etc.). Thus, such consumption and its related CO_2 emissions should be effectively accounted for.

2.5. Auxiliary equation for cost allocation in dissipative devices

For dissipative components such as vacuum condenser and cooling water (CW) heat exchangers, all the costs associated with their internal irreversibilities and exergy consumption are charged directly to the component(s) served by it [44]. Since the unit exergy cost of the cooled stream remains constant through the dissipative components (extraction criterion), the cost of the exergy loss is calculated as in Eq.(7):

$$\dot{C}_{Loss} = c\left(B_{Condesate}^{Hot} - B_{Condesate}^{Cold}\right) + \dot{C}_{abat} \tag{7}$$

where $\dot{C}_{abat}$ is the cost of the auxiliary exergy consumption to operate the dissipative component (e.g., cooling water pump and tower fan driving), and $B_{Condesate}^{Hot}$, $B_{Condesate}^{Cold}$ are the exergy of the hot inlet and cold outlet condensate, respectively.

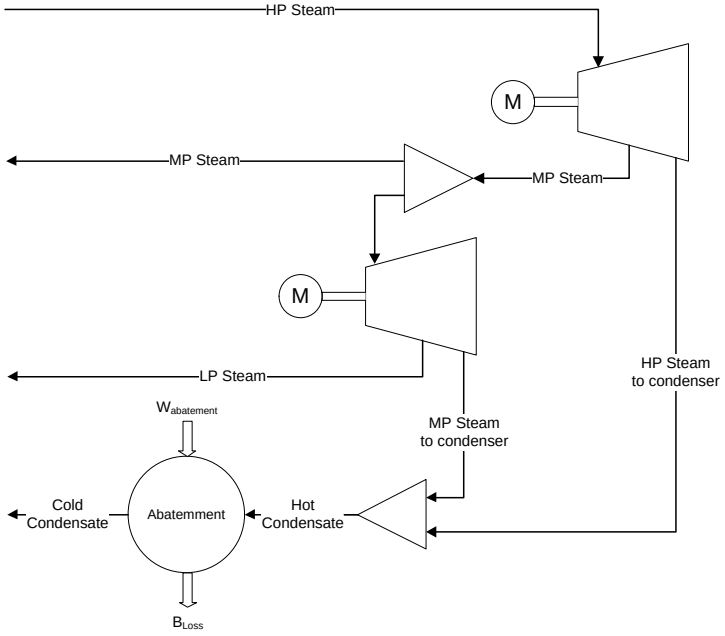

Fig. 5. Cost allocation in dissipative components.

The objective of the condenser is considered to lower the output pressure of the steam turbines [61], thus, the cost of the exergy loss within this dissipative component is allocated to the products of the extraction high pressure (HP) and medium pressure (MP) steam turbines (Fig. 5). The apportioning of the cost of the exergy loss among the products of both steam turbines is based on the amount of exergy dissipated in the condenser unit, $B_{to\,Cond.}^{HP\,Steam}$ and $B_{to\,Cond.}^{MP\,Steam}$ as shown in Eqs.(8-9):

$$\dot{C}_{Loss}^{HP} = \frac{B_{to\,Cond.}^{HP\,Steam}}{\left(B_{to\,Cond.}^{HP\,Steam} + B_{to\,Cond.}^{MP\,Steam}\right)} \cdot \dot{C}_{Loss} \qquad (8)$$

$$\dot{C}_{Loss}^{MP} = \frac{B_{to\,Cond.}^{MP\,Steam}}{\left(B_{to\,Cond.}^{HP\,Steam} + B_{to\,Cond.}^{MP\,Steam}\right)} \cdot \dot{C}_{Loss} \qquad (9)$$

These values are considered as input costs in the cost balances of the respective steam turbine.

2.6. Exergy efficiency of representative equipment

The proposition of a general exergy efficiency definition for the various equipment and units of the integrated syngas and ammonia production plant is not straightforward. This is due to the high transit of chemical and physical exergies of fuel (natural gas), process gas (syngas), solvents and inert streams involving a variety of chemical components, as well as due to the differences in process conditions and product specifications of those facilities. Moreover, even though many works on exergy efficiency calculation claim to effectively measure the exergy transformation ratio of a process in question, an overview on literature points out that the characterization of the exergy performance is often open to interpretations and, in some cases, remains undefined for specific units and conditions [36, 42, 62, 63]. This, consequently, leads to confusions when various processes are compared under different metrics in a quantitative manner, rendering necessary to explain which efficiency definition is adopted. Proposed exergy efficiencies can be classified in mainly two types: (i) *input-output*, and (ii) *consumed-produced* efficiencies, and terms such as ‘exergy input’, ‘exergy output’, ‘exergy loss’, ‘fuel’, ‘exergy expenditure’, ‘useful product’, ‘non-exergetic raw feed’ or ‘transit exergy’ are inherent to them. The first type of such definitions considers the ratio between all the exergy flows leaving the system and exergy flows fed to it, whereas the second type attempts to differentiate the exergy effectively consumed (or produced) by the system from the transit exergy by calculating the exergy change of specific streams on the way to product. Notwithstanding its simple formulation, the *input-output* exergy efficiency may provide misleading results as it deceptively assume a value close to one, for operations which, from an engineering point of view, have a poor performance [64]. In fact, its sensitivity is reduced as the amount of untransformed components increases and thus, as suggested by [42], this approach may rather be successfully

applied when the system consists of a large number of unit operations. Table 1, Eqs.(10-21), summarize the *consumed-produced* exergy efficiency definitions used in this work for representative components of the ammonia plant and a comparison with the simpler *input-output* efficiencies is provided. When defining these formulations, the increase (or decrease) of the chemical exergy between specific input and output streams is considered as a first contribution to the exergy product (or consumption) of the respective unit. Similarly, the increase (or decrease) of the physical exergy of the product compared to that of the feed stream is regarded as a useful exergy output (or expenditure). Other contributions such as power and heat interactions are also accounted for as produced or consumed exergy rates when necessary. Differently from internal losses, arisen from the internal irreversibilities of the actual process (finite driving forces, dissipative process), external losses (e.g. heat loss, exhausted gas, cooling water) are owed to exergy flows intentionally rejected to the environment, and thus, should be subtracted from the exiting exergy [36].

Table 1. Exergy efficiency definitions for representative equipment and units. Tot: Total exergy, CH: Chemical exergy, PH: Physical exergy.

	Exergy efficiency	
Unit (Eq.)	**Input-Output (a)**	**Consumed-Produced (b)**
Combustion Furnace (10)	$\eta_{Furnace} = 1 - \frac{B_{Dest,\,Furnace}}{B^{CH}_{Fuel\,(NG)}}$	$\eta_{Furnace} = \frac{B^{PH}_{Comb.Gases} - B^{PH}_{Comb.Air}}{B^{CH}_{Fuel\,(NG)}}$
Primary reformer (11)	$\eta_{1°\mathrm{Ref}} = 1 - \frac{B_{Dest,\,1°\mathrm{Ref}}}{\left(B^{Tot}_{1°\mathrm{Ref}} + B^{Tot}_{Comb.Gases}\right)}$	$\eta_{1°\mathrm{Ref}} = \frac{\left(B^{CH}_{1°\mathrm{Ref\ Prod}} - B^{CH}_{1°\mathrm{Ref\ Feed}}\right) + \left(B^{PH}_{1°\mathrm{Ref\ Prod}} - B^{PH}_{1°\mathrm{Ref\ Feed}}\right)}{\left(B^{PH}_{Comb.Gases} - B^{PH}_{Hot\,Gases\,0}\right)}$
Secondary reformer (12)	$\eta_{2°\mathrm{Ref}} = 1 - \frac{B_{Dest,\,2°\mathrm{Ref}}}{\left(B^{Tot}_{2°\mathrm{Ref\ Feed}} + B^{PH}_{\mathrm{ProcessAir}}\right)}$	$\eta_{2°\mathrm{Ref}} = \frac{B^{PH}_{2°\mathrm{Ref\ Prod}} - B^{PH}_{\mathrm{ProcessAir}} - B^{CH}_{1°\mathrm{Ref\ Prod}}}{\left(B^{CH}_{1°\mathrm{Ref\ Prod}} - B^{CH}_{2°\mathrm{Ref\ Prod}}\right)}$
HTS (13)	$\eta_{HTS} = 1 - \frac{B_{Dest,\,HTS}}{\left(B^{Tot}_{HTS\,Feed}\right)}$	$\eta_{\mathrm{HTS}} = \frac{B^{PH}_{\mathrm{HTS\,Prod}} - B^{PH}_{\mathrm{HTS\ Feed}}}{\left(B^{CH}_{\mathrm{HTS\ Feed}} - B^{CH}_{\mathrm{HTS\,Prod}}\right)}$
LTS (14)	$\eta_{LTS} = 1 - \frac{B_{Dest,\,LTS}}{\left(B^{Tot}_{LTS\,Feed}\right)}$	$\eta_{\mathrm{LTS}} = \frac{B^{PH}_{\mathrm{LTS\,Prod}} - B^{PH}_{\mathrm{LTS\ Feed}}}{\left(B^{CH}_{\mathrm{LTS\ Feed}} - B^{CH}_{\mathrm{LTS\,Prod}}\right)}$
Steam drum (15)	$\eta_{SD} = 1 - \frac{B_{Dest,\,SteamDrum}}{\left(B^{Tot}_{2°\mathrm{Ref\ Prod}} + B^{Tot}_{BFW_{\bullet Utilities \bullet NH_3Loop}}\right)}$	$\eta_{\mathrm{SD}} = \frac{\left(B^{PH}_{BoilerSteam} - B^{PH}_{BFW_{\bullet Utilities \bullet NH_3Loop}}\right)}{\left(B^{PH}_{2°\mathrm{Ref\ Prod}} - B^{PH}_{\mathrm{HTS\,Feed}}\right)}$
Absorber (16)	$\eta_{Absorb} = 1 - \frac{B_{Dest,\,Absorb}}{\left(W_{\bullet \mathrm{DEAminePump} \bullet \mathrm{DEAmineCooling}} + B^{Tot}_{\bullet \mathrm{ShiftProd} \bullet \mathrm{DEAmine\text{-}to\text{-}CW}}\right)}$	$\eta_{Absorb} = \frac{\left(B^{Tot}_{\mathrm{RichDEA\ to\ L/R\ H.Exch}} - B^{Tot}_{\mathrm{DEAmine\ to\text{-}CW}}\right)}{W_{\mathrm{DEAminePump\ DEAmineCooling}} + \left(B^{Tot}_{\mathrm{ShiftProd}} - B^{Tot}_{\mathrm{Purified\ Syngas}}\right)}$
Desorber (17)	$\eta_{Desorb} = 1 - \frac{B_{Dest,\,Desorb}}{\left(B_{\mathrm{DesorbFeed}} + W_{\bullet \mathrm{Reflux\text{-}CW} \bullet CO_2 gas\text{-}CW} + B^{PH}_{\mathrm{LPSteam}}\right)}$	$\eta_{Desorb} = \frac{\left(B^{Tot}_{\mathrm{Lean\ DEAmine}} + B^{Tot}_{CO_2\ to-Compr} - B^{Tot}_{DesorbFeed}\right)}{W_{\bullet \mathrm{Reflux\text{-}CW} \bullet CO_2 gas\text{-}CW} + \left(B^{PH}_{\mathrm{LPSteam}} - B^{PH}_{LPCond}\right)}$
Ammonia converter (18)	$\eta_{Converter} = 1 - \frac{B_{Dest,\,Converter}}{B^{Tot}_{\mathrm{Reactor\ Feed}}}$	$\eta_{\mathrm{HTS}} = \frac{B^{PH}_{\mathrm{Reactor\,Prod}} - B^{PH}_{\mathrm{Reactor\ Feed}}}{\left(B^{CH}_{\mathrm{Reactor\ Feed}} - B^{CH}_{\mathrm{Reactor\,Prod}}\right)}$

	Exergy efficiency	
Unit (Eq.)	**Input-Output (a)**	**Consumed-Produced (b)**
Utilities plant (19)	$\eta_{Utilities} = 1 - \frac{B_{Dest,\,Utilities}}{B^{PH}_{HP\,Steam} + W_{\substack{\bullet LP\,Pump \\ \bullet HP\,Pump}} + W_{Cond-CW}}$	$\eta_{Utilities} = \frac{W_{\substack{\bullet HPI,HP\,II \\ \bullet MPI,MP\,II}} + B^{PH}_{\substack{\bullet MP\,Steam \\ \bullet LP\,Steam}}}{B^{PH}_{HP\,Steam} + W_{\substack{\bullet LP\,Pump \\ \bullet HP\,Pump}} + W_{Cond-CW}}$
Refrigeration cycle (20)	$\eta_{\mathrm{Refrig}} = 1 - \frac{B_{Dest,\,\mathrm{Refrig}}}{W_{\substack{\bullet Comp\,I \\ \bullet Comp\,II}} + W_{\substack{\bullet Inter-CW \\ \bullet Condser}} + B^{Q}_{Evap}}$	$\eta_{\mathrm{Refrig}} = \frac{-Q_{\mathrm{Evap}}(1 - T_0/T_{Evap})}{W_{\substack{\bullet Comp\,I \\ \bullet Comp\,II}} + W_{\substack{\bullet Inter-CW \\ \bullet Condenser}}} = \frac{COP_{\mathrm{actual}}}{COP_{\mathrm{Carnot}}}$
Cryogenic Purge Gas Treatment (21)	$\eta_{\mathrm{CryoPG}} = 1 - \frac{B_{Dest,\,\mathrm{CryoPG}}}{B^{Tot}_{\substack{AmmoniaFree \\ PurgeGas}}}$	$\eta_{\mathrm{CryoPG}} = \frac{B^{PH}_{\substack{LP\,H_2-N_2 \\ mixture}} + B^{PH}_{\substack{HP\,H_2-N_2 \\ mixture}} + B^{PH}_{FuelGas}}{B^{PH}_{\substack{AmmoniaFree \\ PurgeGas}}}$

According to Eq.(10b), the combustion chamber aims to increase the thermal exergy difference between the products and the reactants at the expense of a fraction of the chemical exergy of the fuel. The same criterion is considered when calculating the exergy efficiency of other exothermic chemical reactors such as secondary reformer, HTS and LTS reactors and ammonia converter Eq.(12b-14b,18b) [65]. So, in the secondary reformer the reactants increase its physical exergy by consuming a part of the chemical exergy in a partial combustion process. In HTS and LTS, the remaining carbon monoxide is consumed, increasing the physical exergy of the process gas, used to preheat the boiler feedwater. For the sake of clarity, it must be warned about the effect of the terms subtracted in the numerators of Eqs. (10b), (12b-14b) and (18b), namely the physical exergy of the input streams. If those terms were considered as exergy inputs and added in the denominator, the calculated value of the exergy efficiency would be drastically modified, owed to the large transiting values of the input physical exergy compared with the chemical exergy difference between input and output streams. On the other hand, the endothermic reactions in the primary reformer aims to increase the total exergy of the process gas stream at expense of the exergy decrease of the hot combustion gases passing through the externally fired reformer to the convection train. The exergy efficiency value for primary reforming obtained in this work is in agreement with the exergy efficiency calculated by other authors using various methodologies [29, 64]. Regarding the CO_2 absorption unit, it is considered that the exergy of the rich DEA solvent increases at the cost of the total exergy decrease of the purified gas in an exothermic reaction. Equation (16b) also includes the exergy losses in the rich DEA throttling and the pumping power and cooling utilities required to the absorption process to operate. Meanwhile, desorber column is responsible for the separation of the chemical components at the expense of (i) the physical exergy supplied to the reboiler, and (ii) the utilities used in the reflux condensation and CO_2 gas cooling process. Thus, its product is the total exergy difference between product and feed streams. It should be also noted that the efficiency of the refrigeration cycle, Eq. (20b), is calculated by considering the exergy of the heat removed at the evaporator temperature. Finally, due to the inexistent chemical reactions and additional power consumptions in the purge gas separation process, the exergy efficiency of the cryogenic purge gas treatment is approximated by calculating the ratio between the physical exergy recovered in the separated products and the amount of exergy fed to the system. Clearly, since a separation process is performed, chemical exergy is affected, but due the large values of transit chemical exergy, its variation is considered negligible if compared with the variation of physical exergy.

3. Results and discussion

The exergy performance and exergoeconomy analysis is highly dependent on the plant operation conditions. Thus, the relevant parameters used to calculate the exergy efficiency and exergy

destruction breakdown in the various units, and to determine the exergy costs and CO_2 emission costs of ammonia and its by-products are briefly presented.

3.1. Process Thermodynamics and Exergy consumption remarks

In this section, the main findings on exergy consumption and thermodynamic performance of the integrated syngas and ammonia plant are presented. It must be noted that these figures correspond to a nominal production capacity of 1000 metric tons/day of ammonia.

- Since no additional exergy input is needed other than the natural gas used as feedstock and fuel in the primary reformer, modern ammonia plants can be considered self-sufficient in terms of steam and power supply [26]. This became possible thanks to an efficient waste heat recovery system that cools down the process gas and recovers part of the exergy of the flue stack gases, so that steam at three levels of pressure can be produced (7, 35, 100 bar). Moreover, as the total enthalpy of ammonia synthesis reaction is about 8.8% (2.718 MJ/tonNH_3) of the total consumption in the ammonia plant, there is a strong incentive in recovering as much as possible of this surplus heat [66]. Even in advanced plants, the mass of steam produced from waste heat is still about 3-4 times than ammonia produced [67]. Steam is consumed (i) in the extraction turbines that drive pumps and gas compressors, (ii) in the desorber reboiler, as well as (iii) a feedstock (MP steam) to the primary reforming (Fig. 6). Total power consumption achieves 22,617 kW.

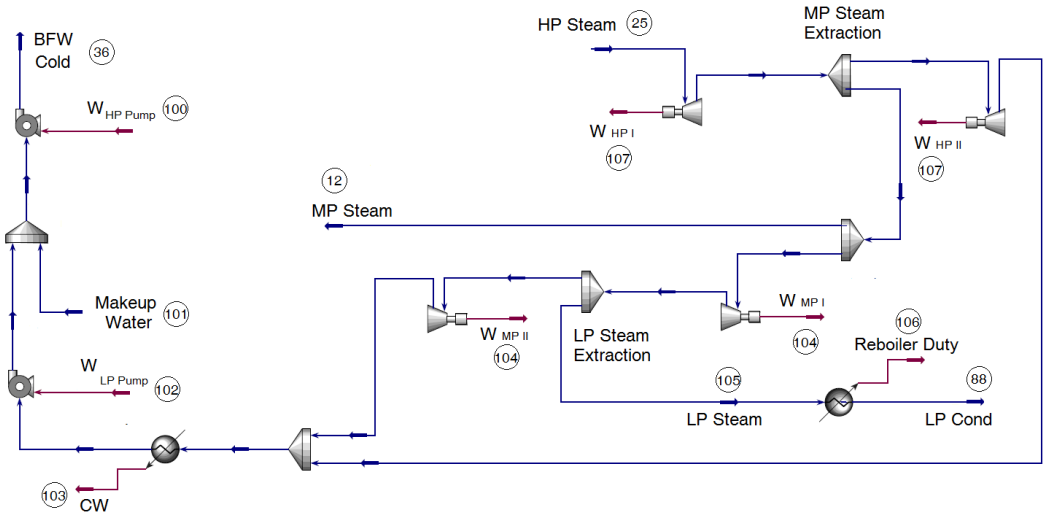

Fig. 6. Utilities plant of the integrated syngas and ammonia production plant.

A mechanical draft cooling tower supplies the cooling water to the condenser as well as for ancillary coolers in a closed circulating system. Cooling tower power consumption, including pumps and fans, is estimated as 833kW [68] and total heat rejection is calculated as 117165 kW [68]. Since that rejected heat leaves the system without being profited anymore, its exergy destroyed. Cooling water inlet and outlet temperatures are set as 40°C and 25°C, respectively. Moreover, due to industrial cooling towers typically have an approach temperature between 5-8°C [69], dry (25°C) and wet bulb (17.9°C) temperatures are assumed for a relative air humidity of 50%. Total volumetric water circulation rate is about 7636.22m^3/h and water make up due to drift, evaporation and blown down are estimated as 2.74% of the circulating water flow. Finally, bottom flash process condensates (15162 kg/h at 35°C) are treated and recovered to the water system. According to Fig. 7a, by far the largest users of cooling water are the condenser and the DEA cooling process, together achieving 55% of the total cooling duty. About one fourth of the cooling duty is used in the ammonia synthesis loop, whereas the desorption unit is responsible for 12.6% of the total cooling. Figure 7b shows the distribution of total plant power utilization. About 42% of the electricity generated is consumed by the syngas compression, followed by the process air compression (28%) and the ammonia refrigeration cycle (12%). The remaining power is used

throughout the plant to drive pumps, compressors, etc. The surplus can be sold to the grid or used in associated urea plants.

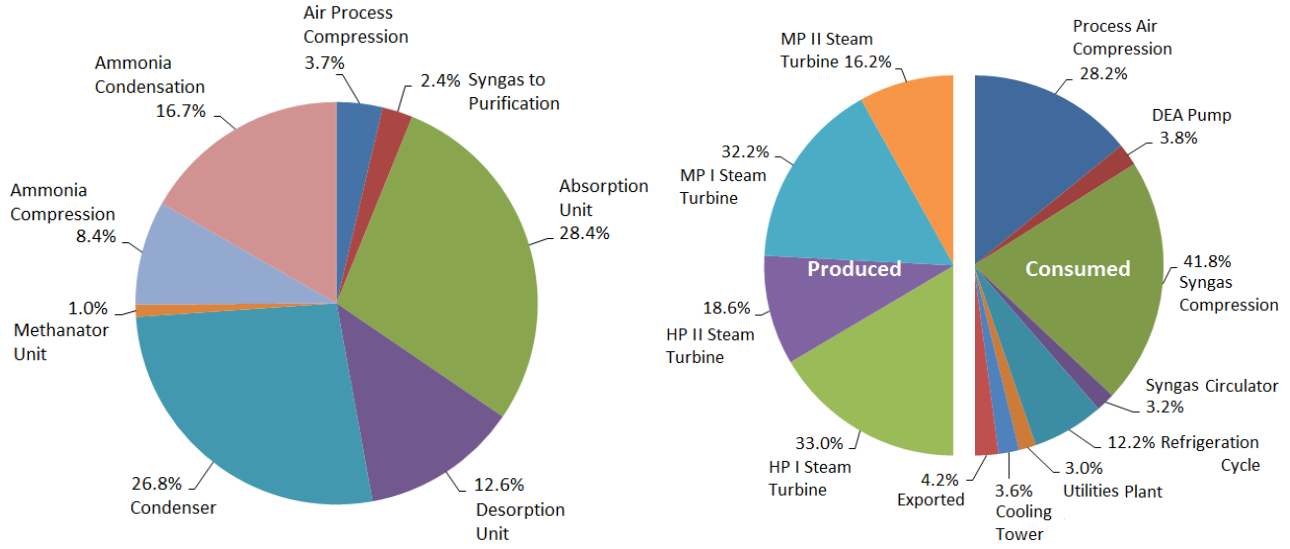

Fig. 7. Distribution of cooling duty (a) and power production/utilization (b) between major users by process. Total cooling duty: 117,165kW; Total power generation: 23,603kW.

- The primary reforming is the most exergy-intensive processes, with a thermal duty of 54,630 kW [70]. Although its endothermic reactions are favored by higher temperatures, mechanical and metallurgical restrictions render the primary reformer heat flux-limited. Besides, according to Le Chatelier principle for increasing-volume reactions, the lesser the reactor pressure, the lesser the methane slip (unreacted methane) [71]. However, considering that further syngas compression is necessary at the front-end of the ammonia loop, a compromise between low methane slip and high syngas pressure is adopted [72]. Thus, reformer operation conditions are limited to 790ºC and 35 bar [33, 73]. Typical steam to carbon ratios (S/C) range from 2.5 to 4.5 depending on feedstock quality, purge gas recovery, reformer capacity, shift operation and plant steam balance [71]. Relatively high S/C ratios (i) shift the equilibrium of reforming reactions to the production of hydrogen, lowering the methane slip; (ii) provide the necessary steam for shift conversion reactions, increasing the H_2 production; as well as (iii) inhibit the occurrence of local overheating and carbon-forming side reactions (methane catalytic decomposition and Boudouard reaction), which could lead to the poisoning of the catalyst [66, 72, 74]. Thus, an S/C ratio of 3.0 is selected as trade-off between excess steam production and methane slip. A lined secondary reformer is used to introduce the nitrogen into the process stream by partially burning with air the remaining methane content at the primary reformer outlet (9%), increasing the syngas temperature (970ºC), and meeting both the required stoichiometric N_2:H_2 ratio and the heat balance [66, 72, 75]. Total air compression power consumption including intercooling achieves 6700kW. The outlet gas is cooled down to a suitable feed temperature for the lined shift reactors, where an additional amount of hydrogen is produced at the expense of the CO and water available in the syngas (9.76% CO, 32.89% H_2O). After the LTS reactor, the CO content has been reduced to less than 1% mol [71].
- Chemical absorption carbon capture system using a 35% wt. in water, di-ethanolamine – DEA [$(HOCH_2CH_2)_2NH$] solution is considered [76, 77]. Chemical exergy of DEA is estimated from the equivalent chemical formula ($C_4H_{11}NO_2$) along with the thermodynamic data and correlations given by [78-80]. DEA solution recirculation rate is about 721 m^3/h, and maximum (rich DEA) and minimum (lean DEA) CO_2 loadings are 0.48 and 0.037 $kmol_{CO2}/kmol_{DEA}$, respectively. The major part of CO_2 gas (99.7%) is chemically absorbed into the solvent, which is stripped at the desorption process. The CO_2 desorption requires a large amount of heat (47,870 kW) fed to the reboiler, which is supplied by low pressure (LP) steam (7 bar, $0.1kg_{Steam}/L_{DEA\ Solution}$) [81, 82]. The calculated heat

load (3.41 MJ/kg_{CO2}) is slightly lower than those reported in literature [83, 84] mostly above 4.0 MJ/kg CO_2, partly explained by the lower enthalpy of reaction and reboiler duty of DEA compared with MEA [33, 85]. Combined, the CO_2 desorber vent (69%) and the reformer stack (21%) emissions achieve 1,757.5 tonCO_2/day (or 1.76tonCO_2/tonNH_3).This is close to 1.87 tonCO_2/tonNH_3 reported in [86], with CO_2 typically compressed and dehydrated for urea production. However, these figures must be revised in light of the exergoeconomy theories and considering ammonia byproducts (e.g. CO_2 gas) also carrying on associated CO_2 emissions.

- Since typical ammonia loop operates at pressures above 150 bar, the syngas leaving the methanation unit must be further compressed in a multi-stage compression system, usually driven by high pressure extraction steam turbines [66]. Syngas compressor and circulator reach a combined power consumption of 10,640 kW. Ammonia synthesis takes place in presence of an iron based catalyst [66] whereby fractional conversions between 10-30% can be achieved. The converter size and loop efficiency are affected by the reactor pressure, the recycled inerts, the feed temperature, the heat removal design and the catalysts. The degree of conversion of H_2-N_2 mixture into ammonia is calculated as 18.97% [23]. Contrary to SMR process, ammonia synthesis is highly exothermic and, as such, maximum equilibrium conversion is temperature-limited, making temperature control desirable either by indirect cooling or direct cold shot [33]. Notwithstanding the equilibrium yield theoretically increases by reducing enough the temperature while increasing reactor pressure [71], the rate of reaction at lower temperatures is extremely low, so rather moderate temperatures must be used to speed up the reaction rate (430ºC) [27, 71]. To achieve a higher synthesis conversion per pass, the build-up of inerts in the recycle gas is controlled by means of a continuous purge of a portion of the hydrogen-rich recycle gas [72, 87, 88]. Since ammonia loop arrangements may differ with respect to the points at which the makeup gas is fed and the ammonia and purge gas are withdrawn [89, 90], the best point for purge gas withdrawal is where the concentrations of inerts are higher, i.e., after the ammonia bulk removal and before the fresh syngas addition [66, 91]. Purge fraction depends on a trade-off between the additional compression power and the wastage of purified hydrogen, and it is set as 7% of total fresh syngas molar flow [92].
- Ammonia condensation is not completely satisfactory if only water or air cooling is performed [71], thus it must be chilled to approx. -20°C by means of a two-stage vapor compression refrigeration system. Ammonia refrigerant offers better properties in terms of heat transfer and power consumption than any other fluid, even CO_2 [93, 94]. However, as it is exhibited by other industrial refrigerants in single-stage compression unit, ammonia experiences a dramatic increase of discharge temperature (> 120°C) which increase the rate of lubricating oil breakdown and the likelihood of compressor material fatigue [95]. Fortunately, high discharge temperatures can be controlled, either by external cooling or by using two-stage compression systems with intercooling [93]. Figure 8 compares two refrigeration systems in which the discharge gas from the low pressure stage compressor is desuperheated by direct contact with vapor or liquid refrigerant. Since vapor from the first throttling process is not passed to the low pressure stage, the quality of ammonia entering the evaporator reduces, improving the refrigeration effect. Besides throttling losses, compression ratios and compression discharge temperature at high pressure stage are also reduced. In case (b), low pressure discharge vapor is mixed with the flashed vapor, instead of passing through the flash tank itself, which results in a slightly superheated inlet condition at high pressure stage compressor. Since cooling water duty and power consumption are higher in case (b), thus case (a) has been adopted. The condenser pressure (13.56bar) is determined by the available cooling water (CW) temperature, which is only justified in large industrial refrigeration systems [96]. Meanwhile, as lower evaporating pressures represent higher compression power, thus an evaporator slightly above ambient pressure is considered (115.2kPa). Both evaporator and condenser operate at a minimum pinch point temperature difference between 5-10ºC.

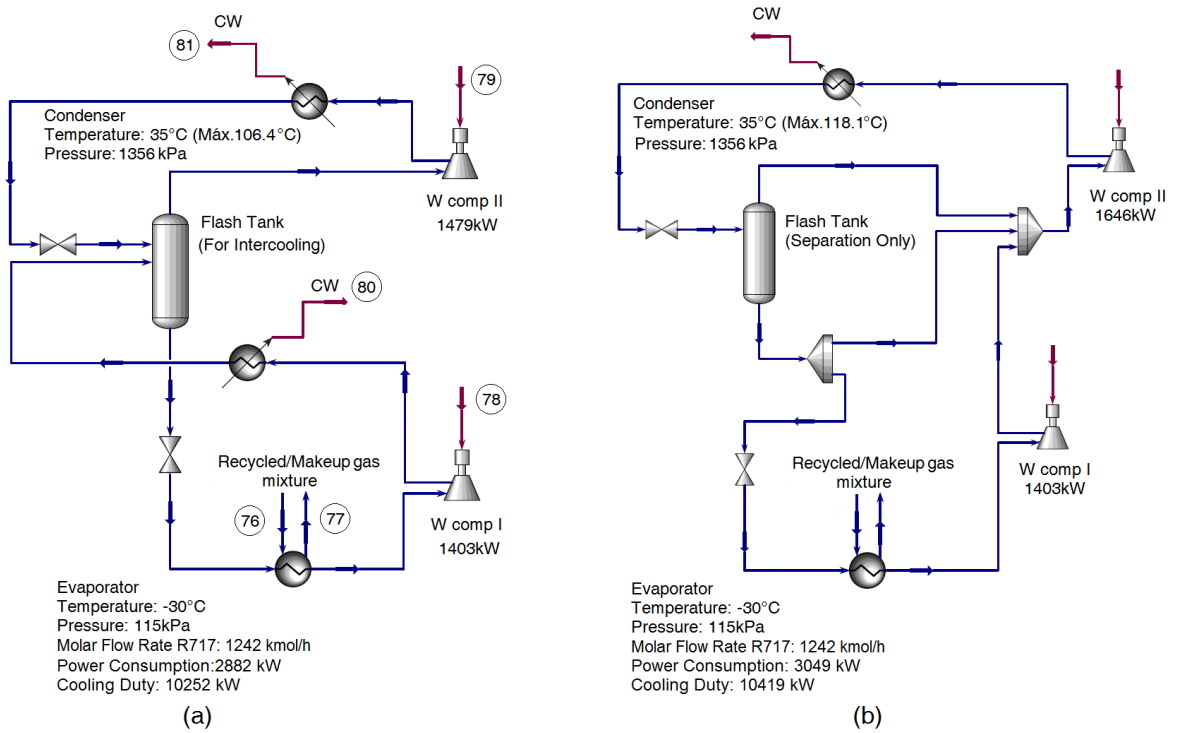

Fig. 8. Multistage ammonia refrigeration systems with flash tank a) as intercooler and b) as vapor separator only.

Figure 9 shows the Temperature vs. Enthalpy diagram for the heat recovery and condensation system of ammonia loop. As expected, the largest temperature differences occur in the converter and the waste heat steam boiler, increasing the exergy destruction on those components.

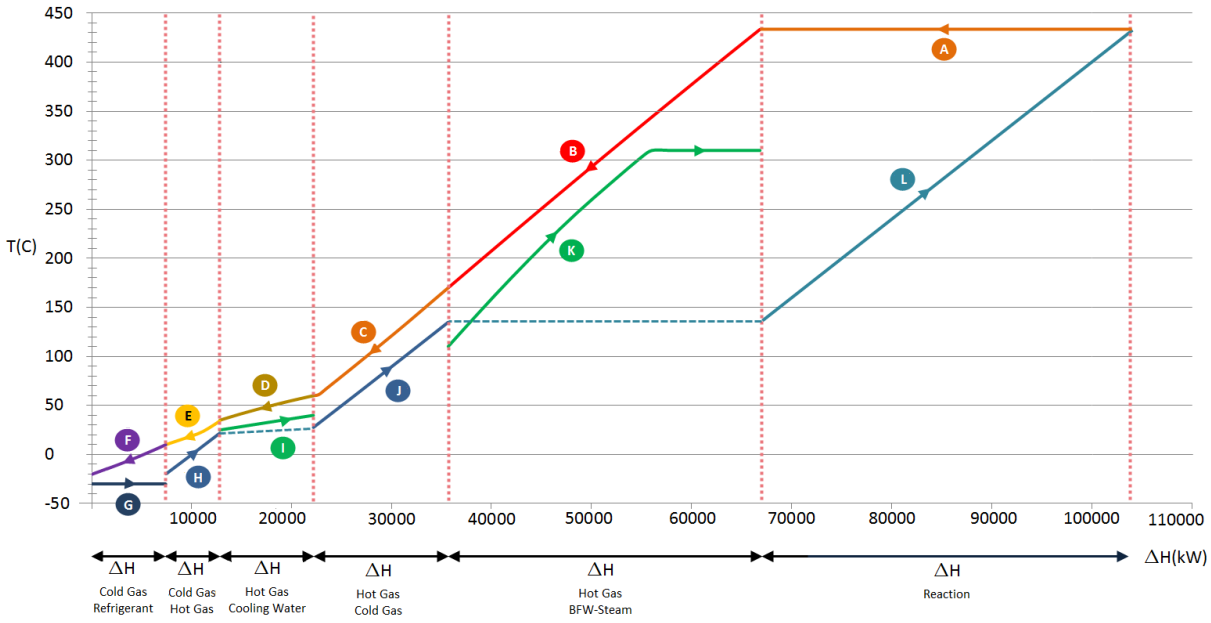

Fig. 9. Temperature - Enthalpy Diagram for Ammonia Loop. Minimum temperature approach 10°C. $\Delta H_{reaction}$ = 32,000kW (47 kJ/mol$_{NH3}$).

- Purge gas normally contains 54% H_2, 23% N_2, and other gases (NH_3, Ar and CH_4) of which hydrogen is the most valuable since it can either be returned to synthesis loop or used as fuel gas [89, 92]. Purge gas water scrubbing removes ammonia and water, otherwise they would solidify downstream. Ammonia is later distilled out of the aqueous mixture [26]. Meanwhile ammonia-free purge gas moisture is removed by means of molecular sieves [26, 89]. In the cryogenic section, an

hydrogen recovery of 94.96% and a nitrogen recovery of 18.54% are achievable at pressures close to ammonia loop pressure [89, 92]. The uncompressed fraction of the hydrogen-rich gas (71bar) could be either externally recompressed and recycled to ammonia loop [87] or used as fuel in the ammonia plant to reduce the feedstock consumption [97]. This process progresses at temperatures below -180°C, suitable to separate almost all the methane and argon in the purge gas [91], and thus they are called cold boxes and the adiabatic condition of the equipment is a decisive factor in the efficiency of the unit.

3.2. Exergy efficiency of representative equipment

Figure 10 shows the exergy efficiency for representative components and units. The causes of the low exergy performance and suitable options for efficiency improvement are discussed below.

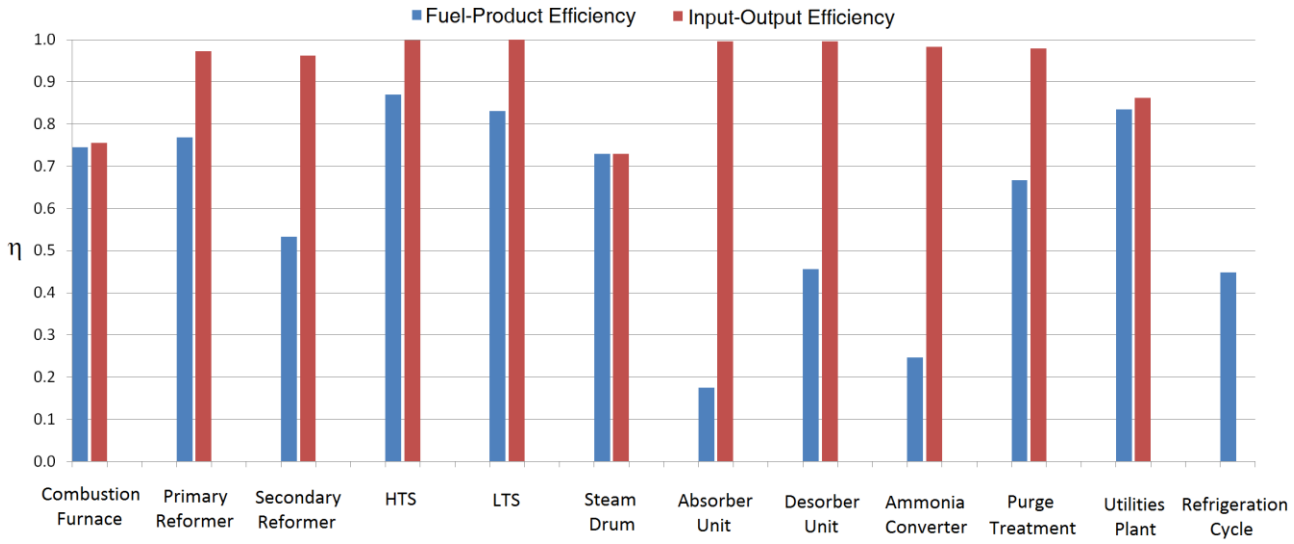

Fig. 10. Exergy efficiency for representative components/unit.

3.2.1. Combustion Furnace and Utilities Plant

The principal irreversible phenomena that occur in heating furnaces and steam boilers are the combustion reactions and the heat transfer between hot gases and heated feed, respectively. Despite the fact that most of the irreversibility due to chemical conversion is inevitable, exergy loss can still be reduced by preheating the reactants [36]. According to Fig. 10, the exergy efficiency of the combustion furnace is slightly higher than that of the boiler; maybe due to the higher mean thermodynamic temperature within the former compared with the steam drum. The exergy efficiency in the steam system can be increased (i) by preheating the boiler feedwater, using the shift reactors effluent; (ii) by raising the mean thermodynamic temperature of the boiler steam and (iii) by superheating the steam in the convection train. The partition of the heat recovery into such steps helps increasing the overall exergy efficiency of the utilities plant. Some authors [31] have reported lower exergy efficiencies of steam generation in a combined heat and power production plant (CHP) when compared with steam production in the energy-integrated chemical plant itself (ammonia, nitric acid and ammonium nitrate), even if some additional fuel must be burnt. For instance, the fuel consumption to generate exported steam in the energy-integrated plant is reported as 10% lower than if steam is produced in a CHP plant operating in the same conditions. Alternatively, a gas turbine coupled to an autothermal reformer (ATR) could be used to provide the heat duty of the reforming process, as well as to produce electricity and process steam in a cogeneration system [98, 99]. In this configuration, no (or less) additional exergy inputs would be required (e.g. natural gas) and, at the same time, the exergy loss due to the steam condensation would be avoided, increasing the overall exergy efficiency. Even though the greatest energy loss in the utilities plants appears in the condenser in the form of rejected heat to the environment, the

exergy loss due to the irreversible process in the condenser and in the cooling water system is, however, relatively small.

3.2.2. Ammonia Converter

Since the exergy associated with unreacted feed or inerts typically constitutes transiting exergy [64], large recycle rates and low conversions in ammonia reactor make its exergy efficiency much lower than that of other exothermic reactors. Higher conversions can be achieved if several reactor beds with optimized intercooling systems and more active catalysts, as well as higher operating pressures are introduced. However, if the converter pressure is increased, the amount of exergy consumed in the circulator and the syngas compressor train is also increased, along with the equipment cost. Moreover, as a decreasing-volume reaction, pressure changes affect the thermodynamics of the ammonia synthesis. As noted by [65], the demands of the Second Law lead to diametrically opposite results when conflicting objectives are aimed to, e.g. reduce the exergy loss (by reducing the driving force of the process) and to increase the process yield (by increasing it). This is the case of the Counteraction and Le Chatelier Principles, both of them used in the design of industrial reactors. For instance, by supposing that all the heat could be isothermally removed as ammonia is produced (e.g. most of the reaction heat is recovered [33]), it can be shown that the exergy efficiency actually increases as pressure is reduced below P_0, according to Eq. (22) [65]:

$$\Delta B^{PH} = \left(n_P - n_R\right) RT_o \ln(P/P_o), \quad \text{for } n_P < n_R \tag{22}$$

This is contrary to Le Chatelier principle, which suggests increasing the pressure of the reactions that decrease in volume, while decreasing the temperature of exothermic reactions to enhance the product yield. To overcome this issue, classical one stage ammonia converters has been superseded by three reactor beds intercooled by waste heat recovery systems producing high pressure steam, whereas novel dual pressure ammonia loops (e.g. Udhe process), that operate by starting at a lower pressures and ending at a higher ones, have claimed higher overall efficiencies. Such improvements aim to increase exergy efficiency but also maintaining high production rates. Recently, so-called heat and mass exchange technologies partially (or completely) replace the syngas feed-to-reactor effluent heat exchanger [100], in which the unseparated ammonia recycled to the converter is reduced at the expense of the enrichment of the effluent stream. Other authors studied the ammonia adsorption in a co-current gas-flowing/solids-fixed bed reactor (GFSFBR) [101], where the removal of the product from the reacting system shifts the equilibrium towards more production of ammonia, as the driving force for the ammonia synthesis remains high in the reactor.

Finally, due to the large power and utilities consumption, the actual coefficient of performance (COP) of ammonia refrigeration achieves 2.43 (compared to 5.42 of reversible Carnot cycle). Clearly, higher conversions will result in the minimization of the recycle rates which lead to both power and utilities savings.

3.2.3. Primary and Secondary Reformers

According to Eq.(22), since the volume of the reacting mixture increases in the primary reforming, $n_P > n_R$, the exergy efficiency increases with higher reformer pressures [65], but also the yield of syngas decreases while methane slip increases [33]. Although some authors [65] have suggested that running an incomplete methane conversion could reduce the exergy expenditure in methane reforming (via Counteraction principle), further methods for separating non-reacted gases in excess would be required (e.g. pressure swing absorption) [102]. To deal with these conflicts, syngas production could be improved by increasing the S/C ratio and the reactor temperature, but it also implies the increase of steam and fuel consumption and the use of costly high temperature resistant materials. Other alternatives, such as a low temperature catalyst pre-reformer at the upstream of primary reformer may help to cut down the reformer fuel consumption about 5-10%, as well as improving the flexibility in terms of the feedstock used in the steam reformer [65]. Further developments such as the Unmixed Reforming (UMR) process [103], the intensified SMR based on micro-channels reactor technology [34], and the chemical looping (CL) reactor producing discrete and pure streams of H_2 and N_2 [104] have been reported to increase steam reforming process

efficiency by decreasing the irreversibilities associated to large driving forces (conversion, heat transfer and mixing).

3.2.4. Syngas Purification

Rich DEA throttling and irreversible heat transfer from lean DEA to cooling water play an important role in the low exergy efficiency of the absorber unit. It is important to point out that, if the effect of DEA cooling and throttling is not included in the efficiency calculation, that value could be as high as 62% instead of 18% shown in Fig 10. On the other hand, the large amount of low pressure steam consumed drops down the exergy efficiency of the desorber unit due to the highly irreversible heat exchange processes occurred in the reboiler and the reflux condenser. According to [65], irreversibility of absorption process can be reduced by reducing absorbent circulation rate and by using two lean absorbent streams each at different optimal CO_2 concentrations (Benfield process). This allows an increase in absorptivity of the solution and avoids the increase of heat consumption of conventional flowsheets.

3.2.5. Cryogenic Purge Gas Treatment

Even though no chemical reactions nor additional power consumption are present in the cryogenic purge gas recovery unit, other dissipative components leads to an exergy efficiency much lower than expected by the simpler *input-output* definition. The throttling process of the cold-box liquid effluent (whereby it partially vaporizes generating the refrigeration driving force) [91] and the large temperature differences between the feed and exit streams in the cryogenic heat exchangers (ranging from 40°C to -191°C) are examples of those components.

3.3. Cumulative unit exergy costs and CO_2 emission cost

The cumulative exergy cost is an indicator of the deviation from thermodynamic perfection encompassing from the natural resources extraction to the final products. Based on the methodology proposed in section 2, and by considering the cumulative unit exergy cost and CO_2 emission cost data for upstream processing stages of natural gas [50] (c_T = 1.1780 kJ/kJ$_{NG}$, c_{NR} = 1.1312 kJ/kJ$_{NG}$, and c_{CO2} = 0.0071 kg$_{CO2}$/MJ$_{NG}$), the total and non-renewable unit exergy costs and CO_2 emission cost of the products of the ammonia plant can be calculated. Table A.2 summarizes the thermodynamic properties and exergy costs calculated for selected streams in the syngas and ammonia production plant. According to these results, ammonia production requires an exergy consumption of 1.7950 kJ per unit of exergy (kJ) of ammonia produced (of which 95.32% correspond to non-renewable sources), equivalent to an ammonia rational exergy production efficiency of 55.71%. Meanwhile, CO_2 emission cost of ammonia produced reaches 0.0881 kg$_{CO2}$/MJ$_{NH3}$, equivalent to 1.69 tonCO$_2$/tonNH$_3$, close to 1.76-1.87 tonCO$_2$/tonNH$_3$ previously reported in section 3.1. The difference between these two values obviously lies in the use of exergy for CO_2 cost allocation among all the products of the plant, instead of charging the CO_2 cost only to the ammonia produced. For instance, the CO_2 production in this plant requires 1.6370 kJ per kJ of CO_2 produced (95.29% coming from non-renewable sources) and carries with a CO_2 emission cost of 0.0821 kgCO$_2$/MJ$_{CO2}$. It shows that the production of ammonia by-products such as hot water, fuel gases and CO_2 gas, widely consumed in associated urea, polymers or methanol production facilities, can also be analyzed in terms of their specific exergy consumption and environmental impact [86]. A comparison with other exergy and energy-based surveys is briefly discussed below. According to Szargut et al. [36] the Cumulative Exergy Consumption (CExC) and the Cumulative Degree of Perfection (CDP) of the ammonia production via the steam reforming of natural gas are 30.9 GJ/t$_{NH3}$ and 64.2%, respectively. Moreover, if an electricity consumption of 0.108kWh per kg$_{NH3}$ is assumed, the CDP would be reduced up to 44.7%. Thus, by considering the exergy of the ammonia, the exergy consumption intensity (1.5574 kJ/kJ$_{NH3}$) and the CO_2 emissions (0.08799 kgCO$_2$/MJ$_{NH3}$) related with the ammonia production can be calculated. However, it must be noted that no apportionment of the exergy costs or the emissions among the various products of the plant is possible without requiring additional assumptions. As pointed out by Szargut et al., unreasonable results could be obtained if the apportioning of the exergy consumption over the useful products in

complex processes is performed on a mass basis. In fact, this approach could be only acceptable if the products are similar (e.g. hydrocarbons distilled from crude oil). The authors also argue that, if the production method is the same for all products, the apportionment of exergy consumption could be based on the exergy values of the useful products. However, since in the present work the considered plant products, namely ammonia, fuel gas, CO_2, hot water, etc. are produced by using different chemical processes throughout various units, the calculation of the exergy costs and the allocation of the CO_2 emissions require a more detailed analysis. Kool et al. [105] reported a world average energy use of ammonia production via steam reforming process as high as 37.5 GJ/t_{NH3} (or in terms of energy intensity, 1.9250 kJ/kJ_{NH3}) whereas the amount of CO_2 emissions allocated only to ammonia is about 0.1102 $kgCO_2/MJ_{NH3}$. Higher values are still possible for coal and oil-fueled plants (up to 60 GJ/t_{NH3}). It is important to notice that these figures are not rationally calculated through a thermoeconomy analysis involving all the plant products, since all the irreversibilities of the processes are charged only to ammonia. In fact, although ammonia synthesis may also generate a net export of either electricity or steam, apart from CO_2, hot water and fuel gas, various surveys deal differently with this co-production. Davis and Haglund [106] considered the steam production to replace the combustion of fossil fuels elsewhere in the life cycle, whereas Ahlgren et al. [107] applies economic allocation for the process products (nitrogen fertilizer and surplus electricity). From a world survey, William and Al-Ansari (2007) calculated an energy-based average specific emission of about 0.1063 kg_{CO2}/MJ_{NH3}, with minimum values as low as 0.0831 kg_{CO2}/MJ_{NH3} [108]. Rafiqul et al. [13] reported an energy-based consumption of 1.7915 kJ/kJ_{NH3} and specific emissions of ammonia production via SMR of about 0.0975kg/MJ_{NH3} in 1995's plants. The theoretical minimum methane consumption for the chemical process of ammonia production is estimated as 22.21 GJ/ton_{NH3} (energy-based) or equivalently as an energy consumption intensity of 1.1195 kJ/kJ_{NH3}, whereas the corresponding CO_2 emissions are reported as 0.0625 kg_{CO2}/MJ_{NH3} [31]. In spite of the several literature reports, none of those studies has allocated the unit exergy costs and CO_2 emissions of the plant among the various products by using an appropriated methodology, misleading the purchasers of ammonia plant co-products to believe they are obtaining low energy-intensive products with reduced emissions. Among the HRCT products, the higher exergy costs correspond to the preheated boiler feedwater and the superheated steam due to the irreversibilities arisen from the large temperature difference between the high temperature combustion gases and the feedwater and saturated steam, respectively. It could be also evidenced in Fig. A.1. Moreover, due to the large amount of power consumed, the exergy costs and CO_2 emissions of the compressed process air are among the highest production and environmental costs in the plant, followed by the low pressure steam used to supply the duty of the stripper reboiler. On the other hand, high and medium pressure steam production present exergy costs of about 1.8000 kJ/kJ_{steam}, and thus, equivalently produced with a rational exergy efficiency of about 55%. The highest proportion of nonrenewable to renewable exergy cost corresponds to steam production (HP steam, MP steam and LP steam), which can be explained by the largest exergy reduction of the combustion gases in the first module of the HRCT (whose exergy input largely comes from natural gas). Such large exergy reduction of the combustion gases also produces a higher allocation of CO_2 emissions to the steam generation process. This approach is more rational than simply allocating the emissions on the products of the last module of the HRCT. It should be noted that higher production costs (15%) are obtained for the power produced in the MP steam turbine when compared to the power produced in the HP steam turbine, which could be explained by the lower temperature and pressure levels of the superheated steam and by the highest contribution of the MP steam turbine condensate (57%) to the heat rejected in the condenser.

It is worthy noticing that this methodology could also be applied to analyze the production of other chemical by-products and valuable surplus heat flow, such as sulfur compounds in refineries, CO_2 production in sugar cane ethanol plants or alternatively, CO_2 injection to revamp oil and gas recovery from depleted reserves [109]. Some authors argue this scheme has the disadvantage of relocating the emission from the plant vent to, for instance, the farmer's field, ultimately ending up in the atmosphere [86]. A greater challenge is the post-combustion CO_2 capture from the primary

reformer stack due to the higher stripping exergy per ton of CO_2, which is higher in comparison to pre-combustion CO_2 capture in ammonia plants [86, 110]. It is also important to notice that, since this first approach deals with a basically fossil-based ammonia production process, the advantages of the cost splitting seem not to be initially so evident. However, reported data on exergy costs and CO_2 emission cost of various fuels [47-51] have shown that a small part of the cumulative unit exergy costs of natural gas and petroleum derivatives corresponds to renewable sources and, thus, it must be accounted for if a fair level playing field for comparative assessments with other syngas and ammonia production technologies is intended. For instance, other scenarios, including the syngas production by using the steam reforming of ethanol, have earned more attention in Brazil, mainly due to its well-established sugar cane ethanol economy [111-115]. Thus, apart from the fossil-based ammonia production process, future works on ethanol-based ammonia production may offer a more interesting opportunity to highlight the importance of the allocation of the renewable unit exergy costs and CO_2 emission cost, including those associated to the upstream processing stages of the sugar cane. Finally, it is emphasized that, even if more stringent environmental policies may demand an additional amount of external (renewable or non-renewable) exergy consumption, the presented methodology would remain applicable, so that the costs of other externalities can also be included.

3.4. Percentage distribution of exergy destruction

As real processes are based on finite-driving forces, they are necessarily irreversible, and a portion of the exergy is always destroyed as the system evolves towards equilibrium. Exergy destruction accounts for the system inefficiencies and gives a useful measure of the way in which resources are consumed and degraded. However, *exergy losses* are not always inevitable and in some cases, a portion of them may be avoided if optimal operation conditions are implemented as the actual process efficiency approaches the exergy efficiency values limited by the *ideal conditions*. In other words, the *exergy analysis* provides a valuable tool that allows comparing the actual and the ideal performance, limiting the technological developments to feasible solutions. Although SNF plants contain many exergy conversion systems, there always exist some major components that dominate the overall exergy performance (reformer, steam boiler, ammonia converter, reboiler, refrigeration cycle, compression train), since the exergy consumption and exergy destruction rates associated with these components are much larger than in the remaining processes [42]. Figure 11 shows the percentage distribution of exergy destruction in the integrated syngas and ammonia production plant and Fig. 12 summarizes the exergy destruction in selected components. The total amount of exergy destruction is 136.48 MW, whereas global exergy consumption is calculated as 405.70 MW. It results in an overall exergy conversion efficiency of 66.36%, close to other values reported via extended exergy costing analysis for ammonia production (from natural gas extraction up to ammonia product) [36]. According to [36], since the exergy of the useful product is much lower than the exergy of the raw materials the exergy efficiency of the process is negative and the Cumulative of the Degree of Perfection is preferred. The main exergy losses are reported in the combustion chamber of the primary reformer and the waste heat boiler. However, since the purge gas is used as fuel instead of recovering the valuable hydrogen contained in it, a significant amount of exergy is destroyed in that study. In any case, the exergy losses of the synthesis gas production unit are much greater than in the ammonia loop process, and some authors [116] have reported that, even though the losses in the ammonia reactor unit decrease by more than 60% by using an optimized synthesis reactor, the exergy losses in a 1,000 tons/day ammonia plant would decrease about only 6% as long as the syngas production unit accounts for more than half of the exergy destruction.

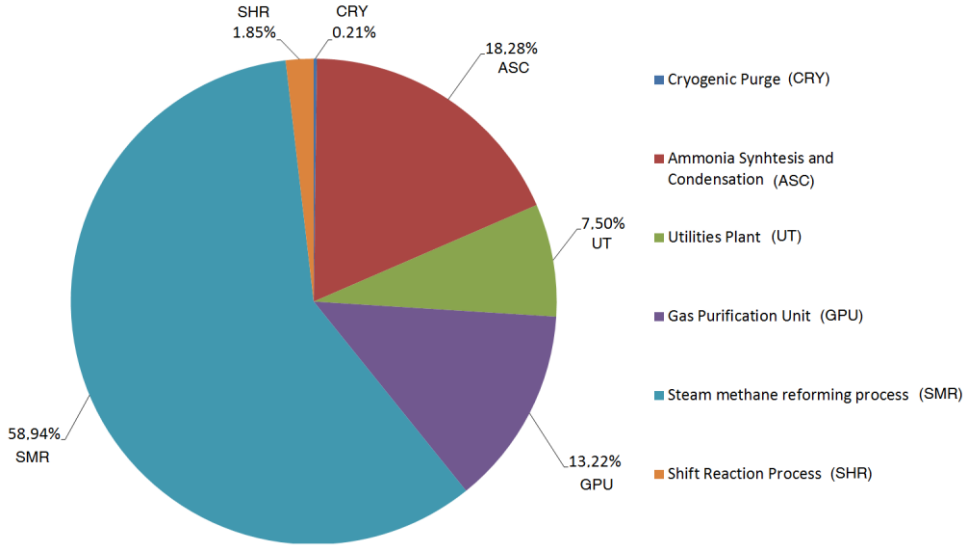

Fig. 11. Breakdown of exergy destruction in the syngas and ammonia production plant. Total exergy destruction: 136.48 MW.

According to Fig. 11, almost 59% of the exergy destroyed corresponds to the reforming section, which includes the highly irreversible fuel combustion in the furnace radiant box. Although in a smaller extent, other processes, such as heat transfer through high finite temperature difference (high driving force) and stream mixing, also represent important sources of exergy destruction in the reforming unit. Regarding the ammonia synthesis loop, it is observed that the highly exothermic ammonia synthesis reaction, the exergy-intensive syngas compression process and ammonia refrigeration, and the large amount of waste heat produced to condensate the ammonia effluent from the reactor are responsible for almost one fifth of the exergy destroyed in the plant. Figure 13 shows the Carnot Efficiency vs. Enthalpy diagram for the ammonia loop, corresponding to the Enthalpy vs. Temperature diagram shown in Fig. 9. In this diagram, the area between the hot composite and cold composite curves represents the exergy destroyed in the ammonia cooling and separation train. As mentioned earlier, better reactor catalysts (such as ruthenium-based catalyst operating at lower pressures) and waste heat recovery systems, alongside better ammonia refrigeration processes may reduce the power consumption, and consequently, exergy destruction in the ammonia loop.

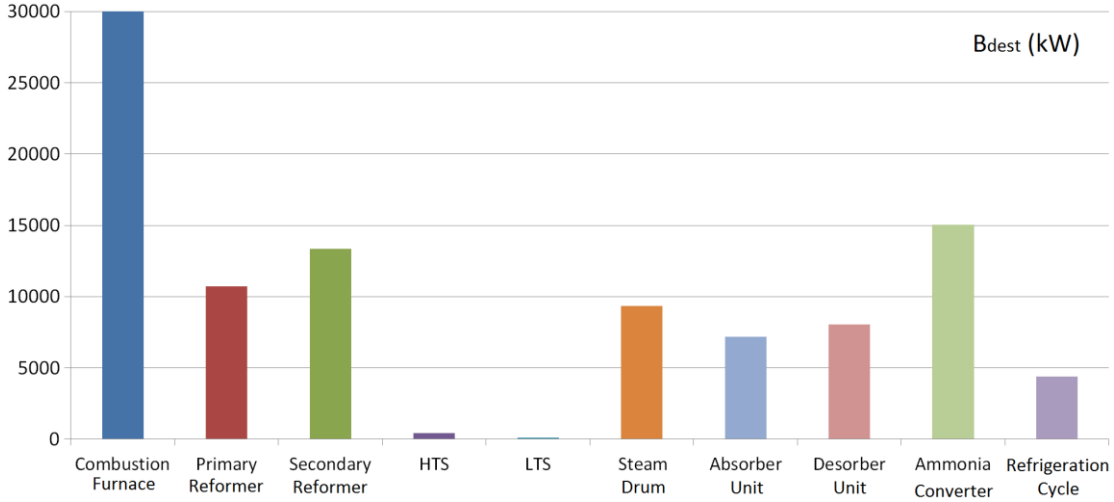

Fig. 12. Exergy destruction rates for selected units.

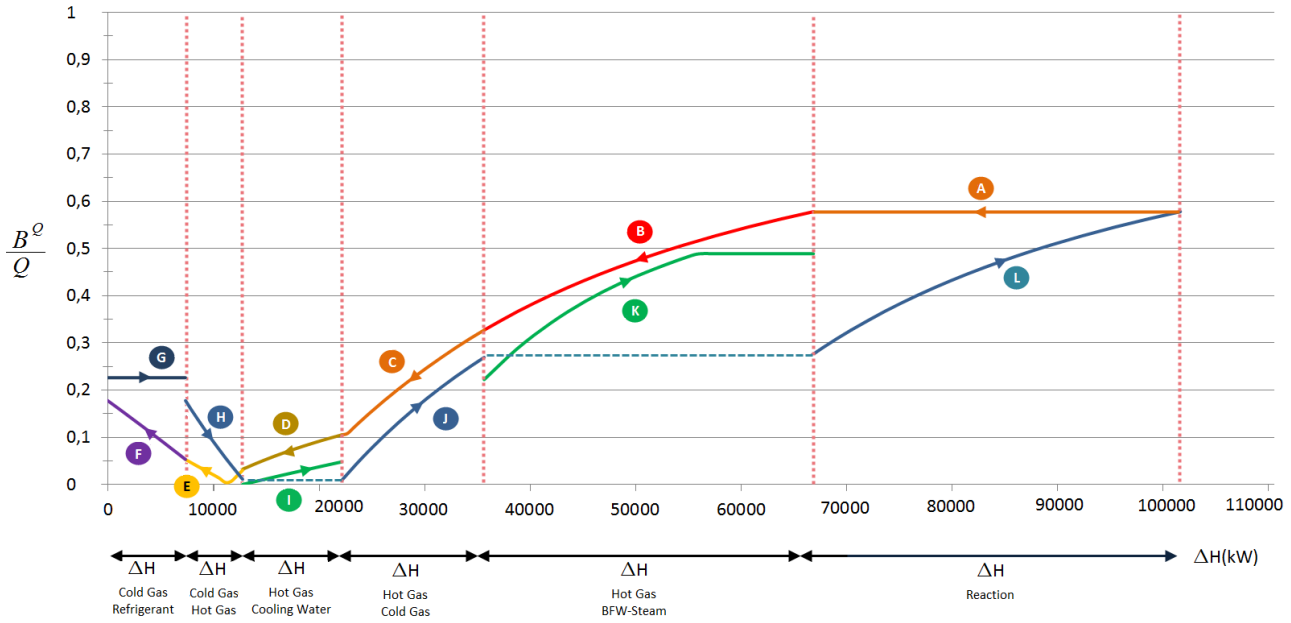

Fig. 13. Carnot Efficiency - Enthalpy Diagram for Ammonia Loop (T in K, and T_o = 298.15 K).
Note: If T_o < 25°C, Carnot efficiency is calculated as $(T_o/T) - 1$.

According to Fig. 12, CO_2 desorption process is one of the main sources of exergy destruction in the ammonia plant (13.22%). Lower steam consumption rates could be achieved by using better available techniques in gas purification systems such as less exergy-intensive chemical (MDEA) or physical solvents. Moreover, it is important to note that gaseous emissions such as flue stack gases and liquid effluents (condensed process steam) are considered as non-treated residues, and as condensate effluent may contain traces of CO_2, ammonia, methanol and amine, further purification process (e.g., steam stripping) could be required depending on environmental regulations [117]. Finally, from Fig. 13, an interesting behavior is shown at the point ammonia is cooled below ambient temperature: the heat exergy associated with cooled stream is actually transferred to the warmer one and, thus, appropriated expressions to calculate exergy efficiencies for process involving cross-ambient temperatures must be used [62].

4. Conclusions

Since co-location of ammonia plants with associated urea, polymers or methanol production facilities is an interesting way to use CO_2 and other ammonia by-products (hot water, fuel gases and CO_2 gas) in a marketable way, it is necessary to evaluate their associated exergy cost and quantify their related environmental impact. Till now, no appropriated methodologies have been developed to address a rational distribution of the exergy costs and CO_2 emission along the convection section of the primary reformer. Thus, a suitable allocation procedure is presented, allowing to attach a zero-unit exergy costs and CO_2 emission cost to the gaseous effluent leaving the primary reformer stack, neither overcharging the last component of the HRCT, nor leaving some cost unallocated. In this way, an ammonia rational production efficiency of 55.71% is obtained, whereas CO_2 emission cost of ammonia produced reaches 0.0881 kg_{CO2} per MJ_{NH3} or 1.69 ton CO_2/ton NH_3. Those figures for CO_2 production are 61.08% and 0.0821 kg_{CO2}/MJ_{CO2}, respectively. It is also verified that the largest share of exergy destruction comes from steam methane reforming process, followed by ammonia synthesis and gas purification unit, with cryogenic purge being responsible for the lowest percentage of exergy destruction in the ammonia plant. On the other hand, calculated reboiler duty (3.41 MJ/kg CO_2) by using DEA is slightly lower compared with MEA explained partly by the lower enthalpy of reaction and higher solvent load. The use of pre-reformers and autothermal reformers are among the more extended strategies adopted to reduce the natural gas consumption and the size of the reformer, even though more complex alternatives have been proposed. Higher

yields could also be achieved if optimized operation conditions, e.g. S/C ratios, pressures and temperatures, and better heat recovery systems and conversion rates are used. Regarding the ammonia loop, better catalysts (higher activities and higher reaction rates at lower pressures), and enhanced converter designs (dual pressure systems, multiple beds) along with improved waste heat recovery and more efficient refrigeration/condensation systems must be pursued if a higher yield and lower exergy destruction is envisaged. However, it is worthy to notice that increasing the driving forces for higher production rates also implies higher exergy destruction rates, according to the Counteraction Principle. Thus, the minimization of the large amount of exergy consumed in the industrial ammonia plants is rather a trade-off between the exergy destruction and high yield rates. Any choice between those conflicting objective functions ultimately will depend on the availability and price of feedstock and project specific conditions. Furthermore, detailed analyses to determine the best alternatives to mitigate its environmental impact are still required showing this field is still open to improvement. Withal, the present results allow identifying the most inefficient, energy intensive and environmentally unfriendly processes, which could be regarded as the starting point of the decision-making for the thermodynamic and thermoeconomy optimization procedures.

Acknowledgments

The first author would like to acknowledge National Agency of Petroleum, Gas and Biofuels – ANP and its Human Resources Program (PRH/ANP Grant 48610.008928.99), and Coordination for the Improvement of Higher Education Personnel (CAPES). Second author would like to thank National Research Council for Scientific and Technological Development, CNPq (grant 306033/2012-7).

Nomenclature

c unit exergy cost (kJ/kJ)
C exergy cost (kW)
c_P specific heat capacity at constant pressure (kJ/kg K)
B exergy rate or flow rate (kW)
BFW boiler feedwater
b specific exergy (kJ/kg)
CW cooling water
E energy (kJ)
E/W electricity (kWh) or mechanical power (kW)
g gravity (9.8 m/s^2)
GHG greenhouse gases
H enthalpy flow rate (kW)
HP high pressure
HRCT heat recovery convection train
HTS high temperature shift
LCA life cycle analysis
LCI life cycle inventory
LHV lower heating value (MJ/kg)
LP low pressure
LTS low temperature shift
M direct CO_2 emissions (kg_{CO2})
MP medium pressure
N, n molar flow (kmol/h)
R_u Universal gas constant
SNF synthetic nitrogen fertilizer
T temperature (°C, K)
t metric ton (1000kg)
v velocity (m/s)

V volume (m^3)
W power (kW)
y molar fraction

Greek symbols

η efficiency
φ ratio between the chemical exergy (b^{CH}) and lower heating value (LHV)
γ activity coefficient

Subscripts and superscripts

abat abatement
C Fuel Consumption
CH chemical exergy
CO_2 carbon dioxide
Comp compressor
CryoPG cryogenic purge gas treatment
Dest destroyed exergy
Evap evaporator
ex exergy
F Processed fuel
HP high pressure
HTS high temperature shift
i i-th stage consumption
Inter-CW intercooling cooling water
k current module of the HRCT
k-1 previous module of the HRCT
K kinetic exergy
Loss Losses
LP low pressure
LTS low temperature shift
n n-th module of the heat recovery convention train
NG natural gas
NR non-renewable
O reference state (298.15 K, 1 atm)
P Produced fuel, Potential exergy (kW)
PH physical exergy (kJ/kg, kW)
Q heat exergy
R renewable
Ref reformer
Ref Prod reformer product
Refrig refrigeration
T Tot total

Appendix A

In natural gas-based ammonia plants about 20-30% of the gas is used as fuel in the combustion furnace and the balance as feedstock in the combustion furnace [26]. After supplying the necessary high level thermal duty to the primary reforming process, flue gas leaving the combustion furnace has still half of its total energy available to be used in the convection train. Table A.1 summarizes the process data of the convection section of primary reformer shown in Figure A.1.

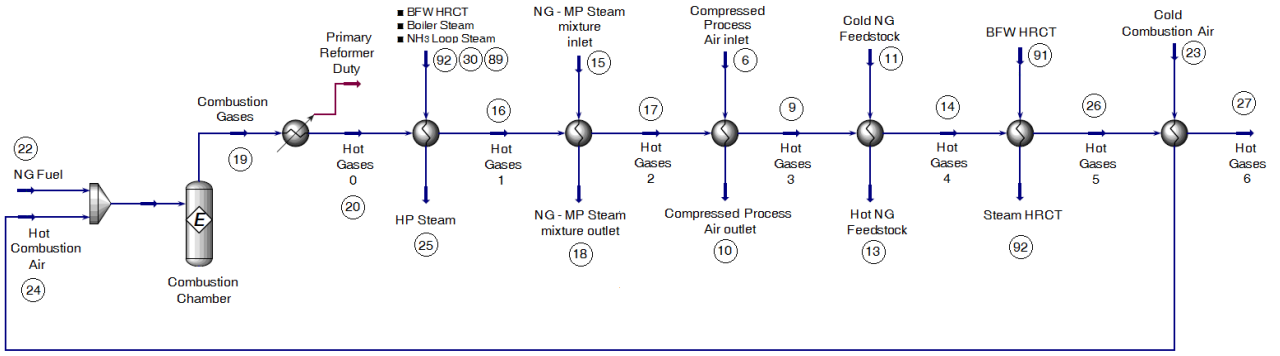

Figure A.1. Convection section of primary reformer.

Table A.1. Process data of the convection section of primary reformer.

Module	n (kmol/h)		T (°C)	P (bar)	B (kW)	c_T (kJ/kJ)	c_{NR} (kJ/kJ)	c_{CO2} (kg_{CO2}/MJ)	Ref Nº
HP steam superheater	10,390	inlet	310	100	60,451	1.5940	1.5260	0.0518	92,30,89
		outlet	460	100	72,505	1.7170	1.6450	0.0524	25
Primary reactor feed preheater	4,800	inlet	361	35	299,844	1.2530	1.2030	0.0109	15
		outlet	580	35	307,714	1.2720	1.2210	0.0115	18
Process air preheater	1,690	inlet	197	35	4,673	3.0980	2.9580	0.0943	6
		outlet	540	35	7,332	2.7390	2.6190	0.0738	10
NG feedstock preheater	1,200	inlet	25	35	280,084	1.1780	1.1310	0.0071	11
		outlet	400	35	282,258	1.1910	1.1430	0.0073	13
BFW heat recovery	1,646	inlet	310	100	4,123	1.8090	1.7240	0.0888	91
		outlet	310	100	9,577	1.8550	1.7740	0.0446	92
Combustion air preheater	5,403	inlet	25	1	0	1.0000	0	0	23
		outlet	310	1	4,054	1.8940	1.7800	0.0047	24

Table A.1 (cont'd.). Process data of the convection section of primary reformer

Stream	n (kmol/h)	T (°C)	P (bar)	B (kW)	c_T (kJ/kJ)	c_{NR} (kJ/kJ)	c_{CO2} (kg_{CO2}/MJ)	Ref Nº
Hot Gases 0	5,919	1287	1	46,953	1.5890	1.5250	0.0254	20
Hot Gases 1	5,919	933	1	29,540	1.5890	1.5250	0.0177	16
Hot Gases 2	5,919	714	1	19,953	1.5890	1.5250	0.0130	17
Hot Gases 3	5,919	628	1	16,487	1.5890	1.5250	0.0096	9
Hot Gases 4	5,919	525	1	12,667	1.5890	1.5250	0.0063	14
Hot Gases 5	5,919	325	1	6,300	1.5890	1.5250	0.0030	26
Hot Gases 6	5,919	82	1	1,651	1.5890	1.5250	0	27

Figure A.2 compares the Enthalpy vs. Temperature and Enthalpy vs. Carnot Efficiency diagrams for the convection train. As it can be seen, higher driving forces (temperature difference) are responsible for the higher exergy destruction in the initial stages of the HRCT.

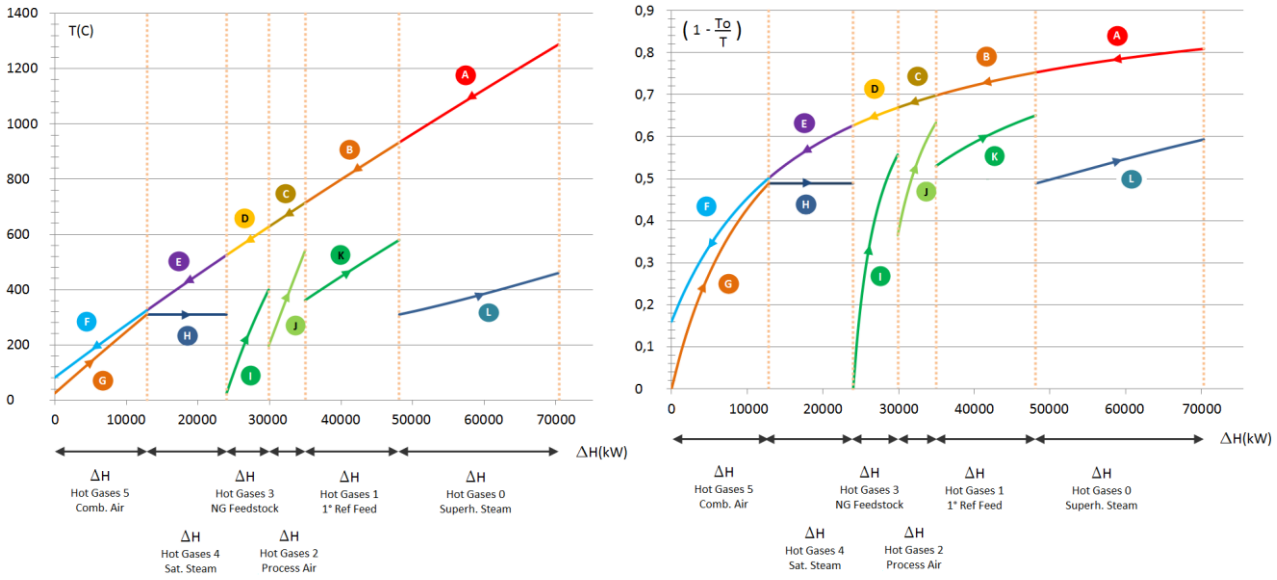

(a) (b)

Figure A.2. Convection section of the primary reformer: (a) Enthalpy-Temperature Diagram. Minimum temperature approach= 14°C; (b) Enthalpy-Carnot Efficiency Diagram (T in K, and T_o = 298.15 K).

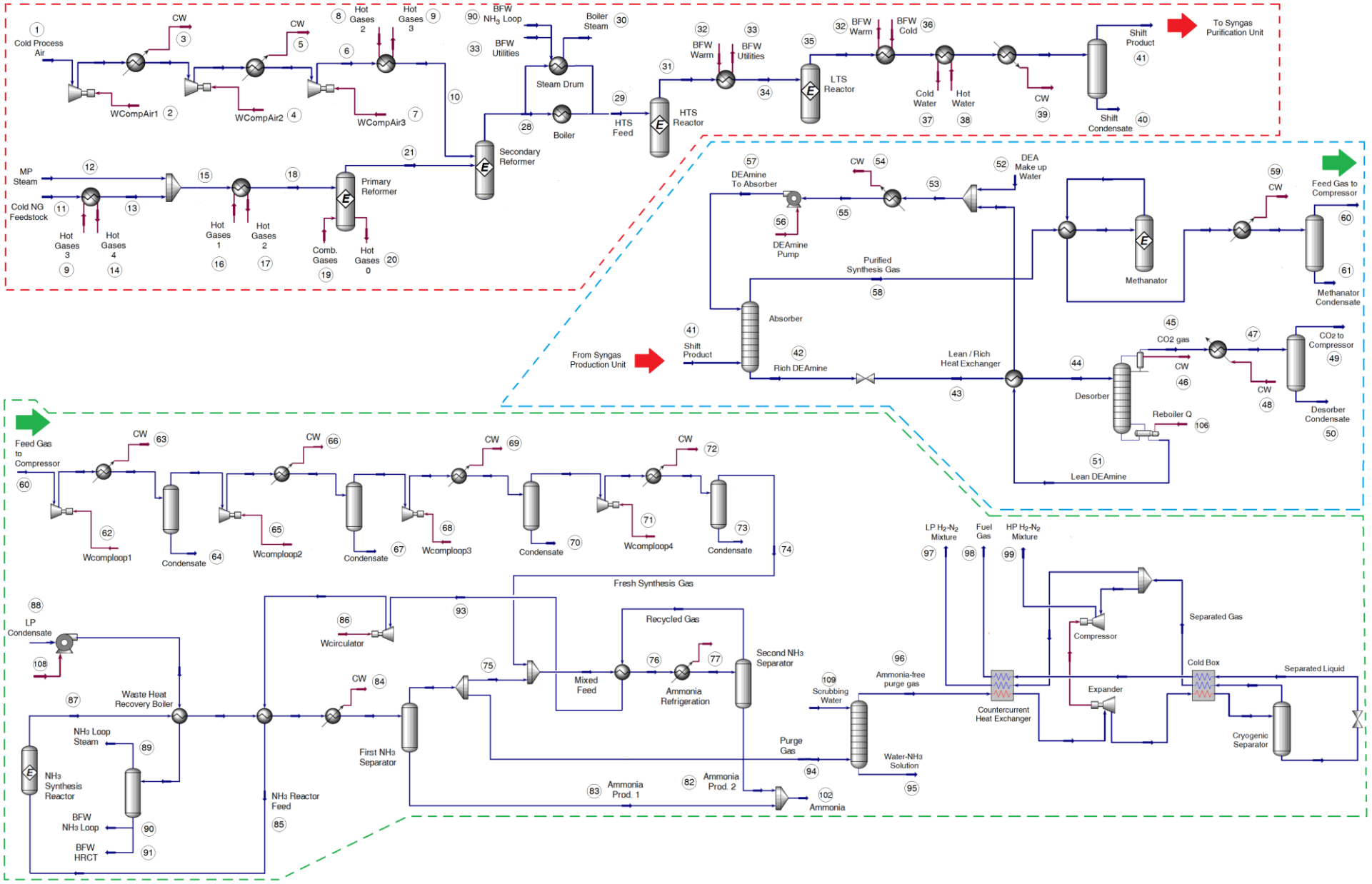
Cold Process Air
CW
WCompAir1
WCompAir2
WCompAir3
Hot Gases 2
Hot Gases 3
BFW NH3 Loop
BFW Utilities
Boiler Steam
Steam Drum
Boiler
HTS Feed
HTS Reactor
BFW Warm
BFW Utilities
LTS Reactor
BFW Warm
BFW Cold
Cold Water
Hot Water
CW
Shift Product
Shift Condensate
To Syngas Purification Unit
MP Steam
Cold NG Feedstock
Hot Gases 3
Hot Gases 4
Hot Gases 1
Hot Gases 2
Primary Reformer
Comb. Gases
Hot Gases 0
Secondary Reformer
DEAmine To Absorber
DEAmine Pump
CW
DEA Make up Water
Purified Synthesis Gas
Absorber
From Syngas Production Unit
Shift Product
Rich DEAmine
Lean / Rich Heat Exchanger
Lean DEAmine
Methanator
Methanator Condensate
Feed Gas to Compressor
CO2 gas
CO2 to Compressor
Desorber
Desorber Condensate
Reboiler Q
Feed Gas to Compressor
Wcomploop1
Condensate
Wcomploop2
Condensate
Wcomploop3
Condensate
Wcomploop4
Condensate
Fresh Synthesis Gas
LP Condensate
Waste Heat Recovery Boiler
NH3 Loop Steam
NH3 Synthesis Reactor
BFW NH3 Loop
BFW HRCT
Wcirculator
NH3 Reactor Feed
First NH3 Separator
Recycled Gas
Mixed Feed
Ammonia Refrigeration
Second NH3 Separator
Purge Gas
Scrubbing Water
Water-NH3 Solution
Ammonia Prod. 1
Ammonia Prod. 2
Ammonia
Ammonia-free purge gas
LP H2-N2 Mixture
Fuel Gas
HP H2-N2 Mixture
Compressor
Countercurrent Heat Exchanger
Expander
Separated Gas
Cold Box
Separated Liquid
Cryogenic Separator

Fig A.3. Detailed layout of the integrated syngas and ammonia production plant.

Table A.2. Selected process data of the integrated syngas and ammonia production plant (1000 metric ton of NH_3 per day).

Ref Nº	Name	n (kmol/h)	T (°C)	P (bar)	B (kW)	c_T (kJ/kJ)	c_{NR} (kJ/kJ)	c_{CO2} (kg_{CO2}/MJ)
1	Cold Process Air	1,690	25	1	0	1.0000	0	0.0000
2,4,7	W_{in} Air Compression	--	--	--	6677	2.153	2.062	0.0657
22	**NG fuel**	**516**	**25**	**1**	**119,203**	**1.1780**	**1.1310**	**0.0071**
11	**NG feed**	**1,200**	**25**	**35**	**4054**	**1.1780**	**1.1310**	**0.0071**
12	**MP Steam**	**3,600**	**350**	**35**	**21,250**	**1.8700**	**1.7910**	**0.0571**
25	**HP Steam**	**10,391**	**460**	**100**	**75,505**	**1.7170**	**1.6450**	**0.0524**
30	Boiler Steam	7,151	310	100	41,599	1.4850	1.4250	0.0452
33	BFW utilities	6,395	297	100	14,477	1.4940	1.4230	0.0777
36	Cold BFW	6,395	30	100	1,977	1.5590	1.0570	0.0337
41	Shift Product	6,512	35	35	285,811	1.4940	1.4230	0.0777
52	DEA makeup water	864	25	1.3	216	1	0	0.0000
42	Rich DEA	30,224	93	2	1,883,324	1.6260	1.5490	0.0819
43	Lean DEA	28,187	111	1.37	1,883,394	1.6370	1.5600	0.0821
56	W_{in} DEA pump	--	--	--	896	2.1530	2.0620	0.0657
60	**Feed gas to Compressor**	**5,279**	**35**	**34.65**	**277,204**	**1.6260**	**1.5490**	**0.0819**
62/65/68/71	W_{in} Syngas Compression	--	--	--	9,883	1.8700	1.7910	0.0571
105	LP Steam	3,997	191	7	16,966	2.1530	2.0620	0.0657
49	**CO_2 to Compressor**	**1,223**	**35**	**1.20**	**6,859**	**1.6370**	**1.5600**	**0.0821**
88	LP Condensate	3,997	109	7	1,882	2.1530	2.0620	0.0657
83	Ammonia Product 1	1,565	35	190	146,627	1.8090	1.7240	0.0888
74	**Fresh Syngas**	**5,271**	**35**	**200**	**284,003**	**1.6530**	**1.5740**	**0.0819**
75	Recycle gas to mixer	10,157	35	190	678,809	1.8090	1.7240	0.0888
93	Feed to circulator	14,478	21.78	190	874,011	1.7710	1.6870	0.0870
94	Purge gas	268	35	190	17,883	1.8090	1.7240	0.0888
91	BFW HRCT	1,646	310	100	4,123	1.8090	1.7240	0.0888
90	BFW NH_3 Loop	756	310	100	1,893	1.8090	1.7240	0.0888
89	NH_3 Loop Steam	1,594	310	100	9,275	1.8090	1.7240	0.0888
82	Ammonia Product 2	950	-20	190	88,469	1.7710	1.6870	0.0870

Ref Nº	Name	n (kmol/h)	T (°C)	P (bar)	B (kW)	c_T (kJ/kJ)	c_{NR} (kJ/kJ)	c_{CO2} (kg_{CO2}/MJ)
95	Aqua ammonia	131	101	190	2,923	1.8370	1.7480	0.0900
99	**HP H_2-N_2 mixture**	**98.5**	**67.2**	**189.6**	**6,313**	**1.8370**	**1.7480**	**0.0900**
97	**LP H_2-N_2 mixture**	**51.9**	**33**	**71**	**3,285**	**1.8370**	**1.7480**	**0.0900**
98	**Fuel Gas**	**85.4**	**12**	**3**	**5,115**	**1.8370**	**1.7480**	**0.0900**
92	Steam HRCT	1,646	310	100	9,577	1.8550	1.7740	0.0446
101	**Makeup water**	**3,600**	**25**	**1**	**900**	**1.0000**	**0**	**0.0000**
107	W_{out} HP turbine	--	--	--	12,189	1.8700	1.7910	0.0571
104	W_{out} MP turbine	--	--	--	11,414	2.153	2.062	0.0657
86	W_{in} circulator	--	--	--	759	1.8700	1.7910	0.0571
109	**Ammonia**	**2,516**	**15**	**190**	**235,014**	**1.7950**	**1.7110**	**0.0881**
--	Makeup CW tower	11,631	25	1	2,908	1.0000	0	0

References

1. Follett, R., Hatfield, J. , *Chapter 4. Utilization and Metabolism of Nitrogen by Humans*, in *Nitrogen in the Environment: Sources, Problems and Management*. 2008, Elsevier USDA-ARS, Soil-Plant-Nutrient Research Unit. p. 720.
2. Erisman, J., Sutton, M., Galloway, J., Klimont, Z., Winiwarter, W., *How a century of ammonia synthesis changed the world.* Nature Geosci, 2008. **1**(10): p. 636-639.
3. Heffer, P., Prud'homme, M. *Fertilizer Outlook 2014-2018*. in *82nd IFA Annual Conference, International Fertilizer Industry Association (IFA), 26-28 May 2014*. 2014. Sydney (Australia).
4. FAO, *World fertilizer trends and outlook to 2018*. 2015: Rome.
5. PETROBRAS. *Fatos e dados: entenda por que investimos em fertilizantes [In Portuguese]*. 2014 14-12-2014]; Available from: http://www.petrobras.com.br/fatos-e-dados/entenda-por-que-investimos-em-fertilizantes.htm.
6. Hernandez, M., Torero, M., *Fertilizer Market Situation: Market Structure, Consumption and Trade Patterns, and Pricing Behavior. IFPRI Discussion Paper 01058*. 2011, International Food Policy Research Institute. p. January 2011.
7. CIESP. *Fertilizantes: Petrobras amplia actuação,12 de maio de 2014 [In Portuguese]*. . 2014 14-05-14]; Available from: http://www.ciesp.com.br/cubatao/noticias/fertilizantes-petrobras-amplia-atuacao.
8. Dias, V., Fernandes, E., *Fertilizantes: Uma Visão Global Sintética.* BNDES Setorial Rio de Janeiro, set. 2006, 2006(24): p. 97-138.
9. Portal.Brasil (2014) *Dilma: "Produzir fertilizante é estratégico para o Brasil" INFRAESTRUTURA, Nitrogenados, 03/05/2014*. Portal Brasil.
10. Worrell, E., Phylipsen, D., Einstein, D., Martin, N.,, *Energy Use and Energy Intensity of the US Chemical Industry*. 2000, Ernest Orlando Lawrence Berkeley National Laboratory: Berkeley, USA.
11. CGEE, *Sustainability of sugarcane bioenergy*, in *Centro de Gestão de Estudos Estratégicos*. 2012: Brasilia, Brasil. p. 360.
12. Alhammadi, H.R., J., *Chapter B4 - Process design and operation: Incorporating environmental, profitability, heat integration and controllability considerations*, in *Computer Aided Chemical Engineering*, S. Panos and C.G. Michael, Editors. 2004, Elsevier. p. 264-305.

13. Rafiqul, I.W., C., Lehmann, B., Voss, A., *Energy efficiency improvements in ammonia production—perspectives and uncertainties.* Energy, 2005. **30**(13): p. 2487-2504.
14. Panjeshahi, M.H., Ghasemian Langeroudi, E., Tahouni, N., *Retrofit of ammonia plant for improving energy efficiency.* Energy, 2008. **33**(1): p. 46-64.
15. Papoulias, S., Grossmann, I., *A structural optimization approach in process synthesis—II: Heat recovery networks.* Computers & Chemical Engineering, 1983. **7**(6): p. 707-721.
16. Papoulias, S., Grossmann, I., *A structural optimization approach in process synthesis—I: Utility systems.* Computers & Chemical Engineering, 1983. **7**(6): p. 695-706.
17. Papoulias, S., Grossmann, I., *A structural optimization approach in process synthesis—III: Total processing systems.* Computers & Chemical Engineering, 1983. **7**(6): p. 723-734.
18. Yee, T.F., Grossmann, I. E., Kravanja, Z., *Simultaneous optimization models for heat integration—I. Area and energy targeting and modeling of multi-stream exchangers.* Computers & Chemical Engineering, 1990. **14**(10): p. 1151-1164.
19. Yee, T.F., Grossmann, I. E., Kravanja, Z., *Simultaneous optimization models for heat integration—III. Process and heat exchanger network optimization.* Computers & Chemical Engineering, 1990. **14**(11): p. 1185-1200.
20. Yee, T.F., Grossmann, I. E., *Simultaneous optimization models for heat integration—II. Heat exchanger network synthesis.* Computers & Chemical Engineering, 1990. **14**(10): p. 1165-1184.
21. Worrell, E., Blok, K., *Energy savings in the nitrogen fertilizer industry in the Netherlands.* Energy, 1994. **19**(2): p. 195-209.
22. Rosen, M.A., *Comparative assessment of thermodynamic efficiencies and losses for natural gas-based production processes for hydrogen, ammonia and methanol.* Energy Conversion and Management, 1996. **37**(3): p. 359-367.
23. Kirova-Yordanova, Z., *Exergy analysis of industrial ammonia synthesis.* Energy, 2004. **29**(12–15): p. 2373-2384.
24. Norskov, J.K., Bligaard, T., Rossmeisl, J., Christensen, C. H., *Towards the computational design of solid catalysts.* Nat Chem, 2009. **1**(1): p. 37-46.
25. Liu, H., *Ammonia Synthesis Catalysts: Innovation and Practice*. Vol. ISBN 978-981-4355-77-3. 2013, Beijing: Chemical Industry Press, ISBN 978-981-4355-77-3.
26. UNIDO, *Fertilizer Manual: UN Industrial Development Organization*. 3rd ed, ed. I.F.D. Center. 1998, Dordrecht, Netherlands: Kluwer Academic Publishers. 616.
27. Chorkendorff, I., Niemantsverdriet, J. W., *Concepts of Modern Catalysis and Kinetics*. 2nd ed. 2007: Wiley-VCH Verlag GmbH & Co, ISBN: 978-3-527-31672-4.
28. Hajjaji, N., Pons, M., Houas, A., Renaudin, V., *Exergy analysis: An efficient tool for understanding and improving hydrogen production via the steam methane reforming process.* Energy Policy, 2012. **42**(0): p. 392-399.
29. Simpson, A., Lutz, A., *Exergy analysis of hydrogen production via steam methane reforming.* International Journal of Hydrogen Energy, 2007. **32**(18): p. 4811-4820.
30. Kirova-Yordanova, Z., *Application of the exergy method to the environmental impact estimation: The nitric acid production as a case study.* Energy, 2011. **36**(6): p. 3733-3744.
31. Kirova-Yordanova, Z., *Thermodynamic Evaluation of Energy Integration and Cogeneration in Ammonium Nitrate Production Complexes.* International Journal of Thermodynamics (IJoT), 2013. **16**(4): p. 163-171.
32. Tock, L., Maréchal, F., Perrenoud, M., *Thermo-environomic evaluation of the ammonia production.* The Canadian Journal of Chemical Engineering, 2015. **93**(2): p. 356-362.
33. Appl, M., *Ullmann's encyclopedia of industrial chemistry, Vol.11. Chapter 2.*, Wiley-VCH, Editor. 2012, Wiley-VCH Verlag GmbH & Co. KGaA, Weinheim.
34. Dopper, J.G., *European Roadmap for Process Intensification*. 2007, Ministry of Economic Affairs: Delft, The Netherlands. p. 53.
35. Ribero, P.H., *Contribution to the Brazilian database for evaluating the life cycle of the synthetic nitrogen fertilizers [In Portuguese]*, in *Chemical Engineering Department, Polytechnic School*. 2009, University of Sao Paulo: Sao Paulo. p. 341.

36. Szargut, J., Morris, D, Steward, F, *Exergy analysis of thermal, chemical, and metallurgical processes*. 1988, New York: Hemisphere Publishing Corporation.
37. Abdollahi-Demneh, F., Moosavian, M., Omidkhah, M., Bahmanyar, H., *Calculating exergy in flowsheeting simulators: A HYSYS implementation.* Energy, 2011. **36**(8): p. 5320-5327.
38. Kotas, T., *The exergy method of thermal planta analysis*. 2 ed. 1995, Malabar, Florida: Krieger Publishing Company.
39. Ayres, R., Warr, B., *Accounting for growth: the role of physical work.* Structural Change and Economic Dynamics, 2005. **16**(2): p. 181-209.
40. Frangopoulos, C.A., *Thermo-economic functional analysis and optimization.* Energy, 1987. **12**(7): p. 563-571.
41. Lozano, M., Valero, A., *Theory of the exergetic cost.* Energy, 1993. **18**(9): p. 939-960.
42. Tsatsaronis, G., *Thermoeconomic analysis and optimization of energy systems.* Progress in Energy and Combustion Science, 1993. **19**(3): p. 227-257.
43. Erlach, B., Serra, L., Valero, A., *Structural theory as standard for thermoeconomics.* Energy Conversion and Management, 1999. **40**(15–16): p. 1627-1649.
44. Lazzaretto, A., Tsatsaronis, G.,, *SPECO: A systematic and general methodology for calculating efficiencies and costs in thermal systems.* Energy, 2006. **31**(8–9): p. 1257-1289.
45. Torres, C., Valero, A., Rangel, V., Zaleta, A., *On the cost formation process of the residues.* Energy, 2008. **33**(2): p. 144-152.
46. Santos, J.C.S., Nascimento, M. A. R., Lora, E. E. S., Reyes, A. M. M, *On the Negentropy Application in Thermoeconomics: A Fictitious or an Exergy Component Flow?* International Journal of Thermodynamics, 2009. **12**(4): p. 163-176.
47. Silva, J.A.M., Flórez-Orrego, D., Oliveira Jr, S., *An exergy based approach to determine production cost and CO2 allocation for petroleum derived fuels.* Energy, 2014. **67**(0): p. 490-495.
48. Silva, J.A.M., Oliveira Jr, S., *An exergy-based approach to determine production cost and CO2 allocation in refineries.* Energy, 2014. **67**(0): p. 607-616.
49. Florez-Orrego, D., Silva, J.A.M., Oliveira Jr, S., *Renewable and Non-Renewable Exergy Cost and Specific CO2 Emission of Electricity Generation: The Brazilian Case.* Energy Conversion and Management, 2014.
50. Florez-Orrego, D., Silva, J.A.M., Velasquez, H., Oliveira, S., *Renewable and Non-Renewable Exergy Costs and CO2 Emissions of Fuels Production for Brazilian Transportation Sector*, in *27th International Conference on Efficiency, Cost, Optimization, Simulation and Environmental Impact of Energy Systems, ECOS 2014, ISBN: 978952-123099-8*. 2014: Turku, Finland.
51. Flórez-Orrego, D., *Comparação Termodinâmica e Ambiental (Emissões de CO2) das Rotas de Produção e Utilização de Combustíveis Veiculares Derivados de Petróleo e Gás Natural, Biocombustíveis, Hidrogênio e Eletricidade (Veículos Elétricos) [In Portuguese]*, in *Department of Mechanical Engineering*. 2014, University of São Paulo: São Paulo. p. 229.
52. Gomes, C., *Thermodynamic, exergetic and thermoeconomic analysis of a thermoelectric powerplant with combined cycle and cogeneration [in Portuguese]*, in *Mechanical Engineering Faculty*. 2001, State University of Campinas: Campinas, Brazil.
53. Silva, M., *Repowering in electricity generation systems in the siderurgic industry [in Portuguese]*, in *Mechanical Engineering Faculty*. 2004, State University of Campinas: Campinas, Brazil.
54. Agudelo, A., Valero, A., Torres, C., *Allocation of waste cost in thermoeconomic analysis.* Energy, 2012. **45**(1): p. 634-643.
55. Borelli, S., Oliveira Junior, S., *Exergy-based method for analyzing the composition of the electricity cost generated in gas-fired combined cycle plants.* Energy, 2008. **33**(2): p. 153-162.
56. Pout, C., Hitchin, R., *Apportioning carbon emissions from CHP systems.* Energy Conversion and Management, 2005. **46**(18–19): p. 2980-2995.
57. Rosen, M., *Allocating carbon dioxide emissions from cogeneration systems: descriptions of selected output-based methods.* Journal of Cleaner Production, 2008. **16**(2): p. 171-177.

58. DEFRA, *2012 Guidelines to Defra / DECC's GHG Conversion Factors for Company Reporting, Departament of Energy and Climate Change* 2012: London.
59. Agudelo, A., Valero, A., Usón, S.,, *The fossil trace of CO2 emissions in multi-fuel energy systems.* Energy, 2013. **58**(0): p. 236-246.
60. Flórez-Orrego, D., Silva, J.A.M., Oliveira Jr, S., *An Exergy and Environmental Comparison of End Use of Vehicle Fuels in Brazilian Transportation Sector.*, in *15th Brazilian Congress of Thermal Sciences and Engineering - ENCIT 2014, November 10-13*. 2014: Belém, PA, Brazil.
61. Silva J.A.M, S., J, Oliveira Jr, S. . ; . p. 1-8, Lausanne, Switzerland. *The condenser product and residues allocation in thermoeconomics*. in *23rd International Conference on Efficiency, Cost, Optimization, Simulation and Environmental Impact of Energy ECOS 2010*. 2010. Lausanne, Switzerland.
62. Marmolejo-Correa, D., Gundersen, T., *A comparison of exergy efficiency definitions with focus on low temperature processes.* Energy, 2012. **44**(1): p. 477-489.
63. Brodyansky, V.M., Sorin, M.V. and Le Goff, P., *The Efficiency of Industrial Processes: Exergy Analysis and Optimization*. 1994, Amsterdam: Elsevier.
64. Sorin, M., Lambert, J., Paris, J., *Exergy Flows Analysis in Chemical Reactors.* Chemical Engineering Research and Design, 1998. **76**(3): p. 389-395.
65. Leites, I.L., Sama, D. A., Lior, N., *The theory and practice of energy saving in the chemical industry: some methods for reducing thermodynamic irreversibility in chemical technology processes.* Energy, 2003. **28**(1): p. 55-97.
66. Tamaru, K., *The History of the Development of Ammonia Synthesis*, in *Catalytic Ammonia Synthesis*, J.R. Jennings, Editor. 1991, Springer US. p. 1-18.
67. Appl, M., *Ammonia: Principles and Industrial Practice*. 1999, New York: Wiley-VCH Verlag.
68. GEA. *Cooling Tower Calculator - GEA Heat Exchangers | GEA Aircooled Systems*. 2008 10-10-14]; Available from: http://www.gea-energytechnology.com/opencms/opencms/gas/en/calculators/.
69. Huchler, L., *Cooling towers part 2: operating, monitoring and maintaining.* Chemical Engineering Progress, 2009. **October**: p. 38-41.
70. Flórez-Orrego, D., Oliveira Jr, S. *On the Allocation of the Exergy Costs and CO2 Emission Cost for an Integrated Syngas and Ammonia Production Plant*. in *28th International Conference on Efficiency, Cost, Optimization, Simulation and Environmental Impact of Energy Systems, ECOS 2015*. 2015. Pau, France.
71. EFMA, *Booklet No. 1 of 8: Production of Ammonia*, in *Best Available Techniques for Pollution Prevention and Control in the European Fertilizer Industry* E.F.M. Association, Editor. 2000: Brussels, Belgium.
72. Maxwell, G., *Synthetic Nitrogen Products: A Practical Guide to the Products and Processes* 2004, New York: Springer US.
73. Meerman, J., Hamborg, E., van Keulen, T., Ramírez, A., Turkenburg, W. C., Faaij, A. P. C., *Techno-economic assessment of CO2 capture at steam methane reforming facilities using commercially available technology.* International Journal of Greenhouse Gas Control, 2012. **9**(0): p. 160-171.
74. Hou, K., Hughes, R., *The kinetics of methane steam reforming over a Ni/-Al2O3 catalyst.* Chemical Engineering Journal, 2001. **82**: p. 311-328.
75. Van Beurden, P., *On the catalytic aspects of steam-methane reforming.* Energy Research Centre of the Netherlands (ECN), Technical Report I-04-003, 2004.
76. Movagharnejad, K., Akbari, M., *Simulation of CO2 Capture Process.* World Academy of Science, Engineering & Technology, 2011(58): p. 192-196.
77. Kohl, A.L., and Nielsen, R.B., *Gas Purification*. 5th ed. 1997: Gulf Publishing Company.
78. Channiwala, S., Parikh, P.,, *A unified correlation for estimating HHV of solid, liquid and gaseous fuels.* Fuel, 2002. **81**(8): p. 1051-1063.
79. Cheremisinoff, N., *Industrial Solvents Handbook, Revised And Expanded, ISBN 9780824740337*. 2003, New Yor, USA: CRC Press. 344.

80. Song, G., Xiao, J., Zhao, H., Shen, L., *A unified correlation for estimating specific chemical exergy of solid and liquid fuels.* Energy, 2012. **40**(1): p. 164-173.
81. DOW, *Gas Sweetening - The Dow Chemical Company. Form No. 170-01395*. 1998, The Dow Chemical Company.
82. Addington, L., Ness. C., *An Evaluation of General Rules of Thumb in Amine Sweetening Unit Design and Operation*, in *GPA Europe Sour Gas Processing Conference*. 2009: Sitges, Spain.
83. Desideri, U., Paolucci, A., *Performance modelling of a carbon dioxide removal system for power plants.* Energy Conversion and Management, 1999. **40**(18): p. 1899-1915.
84. Oi, L.E., *Aspen HYSYS Simulation of CO2 Removal by Amine Absorption from a Gas Based Power Plant*, in *SIMS2007 Conference*. 2007: Goteborg, Sweden
85. Polasek, J., Bullin, J. *Selecting Amines for Sweetening Units, Process Considerations in Selecting Amine*. in *Proceedings GPA Regional Meeting*. 1994. Tulsa, OK: BRE - Bryan Research and Engineering, Inc. - Technical Papers.
86. Strait, R., Nagvekar, M., *Carbon dioxide capture and storage in the nitrogen and syngas industries.* Nitrogen+Syngas. January-February 2010, 2010(303).
87. Howell, J., *The Membrane Alternative: Energy Implications for Industry: Watt Committee Report Number 21*. 1990, New York, USA: CRC Press
88. Schendel, R.L., Mariz, C.L., Mak, J.Y., *Is permeation competitive?* Hydrocarbon Process, 1983. **62**(58).
89. Kent, J., *Handbook of Industrial Chemistry and Biotechnology*. 12th ed. Vol. 1. 2012.
90. IPTS, *Reference Document on Best Available Techniques for the Manufacture of Large Volume Inorganic Chemicals - Ammonia, Acids and Fertilisers Industries*. 2007, Integrated Pollution Prevention and Control
91. Ostuni, R., Filippi, E., Skinner, G.F., *Hydrogen and Nitrogen Recovery from Ammonia Purge Gas. US20130039835 A1*. 2013, Ammonia Casale Sa.
92. Isalski, W.H., Tomlinson, T.R., *Expansion and compression using work generated in expansion. US4312851 A*. 1982, Isalski Wieslaw H, Tomlinson Terence R.
93. Pearson, A., *High Pressure Ammonia Systems – New Opportunities* in *International Refrigeration and Air Conditioning Conference, July 12-15, 2010. Paper 1111*. 2010, Purdue Unviversity: Purdue, USA.
94. Smith, R., *Chemical Process: Design and Integration*. 2005, Manchester: Wiley and Sons.
95. Jekel T. B., R.D.T., *Single-or two-stage compression.* ASHRAE Journal, 2008. **50**(8): p. 46-51.
96. Ludwig. P.E, E.E., *Chapter 12 Compression equipment (Including Fans)*, in *Applied Process Design for Chemical & Petrochemical Plants*, E.L. Ernest, Editor. 2001, Gulf Professional Publishing. p. xi-xii.
97. Mukhopadhyay, M., *Fundamentals of Cryogenic Engineering*. 2010, Delhi: PHI Learning Pvt. Ltd.
98. Knopf, C., *Modeling, Analysis and Optimization of Process and Energy Systems, 1st Ed.* 1st Ed. ed. 2011: Wiley, ISBN: 978-0-470-62421-0.
99. Alves, L., Nebra, S. *Exergoeconomic analysis in hydrogen production by Autothermal reforming of natural gas with Cogeneration*. in *22nd International Conference on Efficiency, Cost, Optimization, Simulation and Environmental Impact of Energy Systems, August 31 – September 3*. 2009. Foz do Iguaçu, Paraná, Brazil: ABCM.
100. Seider, W., Seader, J., Lewin, D., *Product Process and Desing Principles: Synthesis, Analysis and Evaluations*. 2nd ed. 2004: John Wiley and Sons. 1122.
101. Nikačević, N., Jovanović, M., Petkovska, M., *Enhanced ammonia synthesis in multifunctional reactor with in situ adsorption.* Chemical Engineering Research and Design, 2011. **89**(4): p. 398-404.
102. Appl, M., *Modern Amonia Technology*. Nitrogen, 1992. **199 (September-October)**(46).
103. Kumar, R., Lyon, R., Cole, J., *Unmixed Reforming: A Novel Autothermal Cyclic Steam Reforming Process*, in *Advances in Hydrogen Energy* C. Padró, Lau, F., Editor. 2002, Kluwer Academic/Plenum Publishers: New York. p. 31-45.

104.Edrisi, A., Mansoori, Z., Dabir, B., *Using three chemical looping reactors in ammonia production process – A novel plant configuration for a green production.* International Journal of Hydrogen Energy, 2014. **39**(16): p. 8271-8282.
105.Kool, A., Blonk, H., *LCI data for the calculation tool Feedprint for greenhouse gas emissions of feed production and utilization: GHG Emissions of N, P and K fertilizer production*. 2012, Blonk Consultants: Netherlands.
106.Davis, J., Haglund, C., *Life Cycle Inventory (LCI) of Fertiliser Production: Fertiliser Products Used in Sweden and Western Europe, SIK-report No. 654*. 1999: Gothenburg, Sweden.
107.Ahlgren, S., Baky, A., Bernesson, S., Nordberg, A., Norén, O., Hansson, P.A., *Ammonium nitrate fertiliser production based on biomass. Environmental effects from a life cycle perspective.* Bioresource Technology, 2008. **99**: p. 8034 - 8041.
108.Haas, M., Dijk, T., *Inventarisatie klimaatvriendelijke kunstmest .Nutriënten management instituut (NMI)*. 2010: Wageningen.
109.Audus, H., Kaarstad, O., Kowal, M. *Decarbonization of fossil fuels: hydrogen as an energy carrier*. in *Proceedings of the 11th World Hydrogen Energy Conference*. 1996. Stuttgart, Germany.
110.CHEMCAD. *Power Plant Carbon Capture with CHEMCAD. rev. 031109. Technical Articles*. Engineering advanced 2009 12-10-14]; Available from: http://www.chemstations.com/content/documents/Technical_Articles/Power_Plant_Carbon_Capture_with_CHEMCAD.pdf.
111.Caetano de Souza, A., Luz-Silveira, J., Sosa, M., *Physical-Chemical and Thermodynamic Analyses of Ethanol Steam Reforming for Hydrogen Production.* Journal of Fuel Cell Science and Technology, 2006. **3**(3): p. 346-350.
112.Silveira, J., Souza, A., Silva, M., *Thermodynamic Analysis of Direct Steam Reforming of Ethanol in Molten Carbonate Fuel Cell.* Journal of Fuel Cell Science and Technology, 2008. **5**(2): p. 021012-021012.
113.BNDES, *Bioetanol de cana-de-açúcar: Energia para o desenvolvimento sustentável*. 2008, Rio de Janeiro: BNDES.
114.Rossi, C., Alonso, C., Antunes, O., Guirardello, R., Cardozo-Filho, L., *Thermodynamic analysis of steam reforming of ethanol and glycerine for hydrogen production.* International Journal of Hydrogen Energy, 2009. **34**(1): p. 323-332.
115.Lima da Silva, A., Malfatti, C., Müller, I., *Thermodynamic analysis of ethanol steam reforming using Gibbs energy minimization method: A detailed study of the conditions of carbon deposition.* International Journal of Hydrogen Energy, 2009. **34**(10): p. 4321-4330.
116.Maansson, B., Andresen, B., *Optimal temperature profile for an ammonia reactor.* Industrial & Engineering Chemistry Process Design and Development, 1986. **25**(1): p. 59-65.
117.Mudahar, M., Hignett, T., *Energy efficiency in nitrogen fertilizer production.* Energy Agric, 1985. **4**: p. 159-177.